In: Book Title
Editor: Editor Name, pp. 1-59

ISBN 0000000000

Chapter 1

MATHEMATICAL MODELS IN MANGROVES INDUCED SOIL SALINIZATION

Gonzalo Galiano *
Dept. of Mathematics, Universidad de Oviedo, Spain

Contents

*E-mail address: galiano@uniovi.es

Key Words: Ecology of mangroves, salinization, Stokes-Darcy flow, Oberbeck-Boussinesq approximation, system of partial differential equations, mixed formulation, existence of solutions, uniqueness of solutions, stability analysis, free boundary problem, dead core, dynamic boundary condition.

AMS Subject Classification: 35Q92, 76S05, 35Q35, 35K55, 35M32, 35A01, 35A02, 35B35, 35B40, 35R35.

Abstract

We introduce a mathematical model expressed in terms of partial differential equations describing the dynamics induced by the mangroves fresh water uptaking mechanisms in a water-soil domain with salt concentration close to that of sea water. The extraction of fresh water by mangrove roots implies the formation of a salt concentration gradient between the roots layer and the surroundings. In particular, an instable density driven situation follows since water density is higher in the root zone than below it, resulting in a net flow of water downward from the soil surface, which carries salt with it. In the absence of lateral flow, the long term salinity profile in the root zone must be such that the salinity around the roots is higher than that of sea water, and that the concentration gradient is large enough so that the advective downward flow of salt is balanced by the diffusive flow of salt back up to the surface.

Based on the above observations, we start the setting of our model by considering a spatial domain splitted in two subdomains: the water and the soil, assumed to be a water saturated porous medium. This situation corresponds, for instance, to the case in which mangrove grow in back waters, swamps or marshes. In each of these subdomains we consider a suitable set of partial differential equations describing the evolution of salt concentration, water discharge, and pressure, e.g., the Oberbeck-Boussinesq Stokes-Darcy approximation for free fluid and porous medium. We study the relationship among the physical parameters (hydraulic conductivity, mangrove transpiration rate, salinity threshold for water uptake, etc.) in each subdomain to set appropriate scales for the problem and then deduce several simpler mathematical models according to the size of the equations coefficients resulting from the rescaling and to the boundary conditions corresponding to different situations of interest. We then prove several mathematical properties of the models such as the existence and uniqueness of solutions, the time convergence of solutions of evolution problems to the steady states, conditions for the stability of the one-dimensional solution and conditions under which solutions attain the threshold salinity level, among others. We also provide numerical simulations of our models based on finite differences and finite elements methods.

1 Introduction

Mangrove ecosystems are tropical or subtropical communities of mainly tree species which can be found on low, muddy, usually intertidal coastal areas. They cover an area of approximately twenty million hectares throughout the world, with the largest expanses occurring in Malaysia, India, Brazil, Venezuela, Nigeria and Senegal [59]. Mangroves communities are of great ecological importance due to the role they play as habitat builders and shoreline stabilizers, among others. They typically grow in saline coastal soils, or muds, which develop through a combination of two processes: mineral sediment deposition and organic matter accumulation. This soil structure in conjunction to the usual flatness of the area and the almost permanent sea water saturation of the soil due to the regular inundation by tides, when not prolonged periods of waterlogging [35], causes a poor soil draining and flushing of the interstitial water.

One of the decisive mangrove capabilities and perhaps the reason for its comparative fitness to the coastal areas is their ability to exclude most of the salt from the water their roots extract from the sea-water saturated soil, [7]. When they do that, the water must flow downwards from the soil surface towards the roots zone, with salt being carried by convection. Since mangroves roots excludes most of the salt, the salinity must rise in the soil occupied by the roots, and must keep rising, until a sufficiently large concentration gradient develops so that the advective downward flow of salt is balanced by the diffusive flow of salt back to the surface.

In the article *Mangroves may salinize the soil and in so doing limit their transpiration rate*, by Passioura, Ball and Knight [47], the authors provide an analytical approach to the mechanisms of soil salinization produced by mangroves and investigate the consequences of salt concentration increase on mangroves transpiration rate. In their work the authors presented one-dimensional (depth) steady state equations governing the flow of salt and uptake of water in the root zone, assuming that there is an upper limit C_1 to the salt concentration at which roots can take up water, and that the rate of uptake of water is proportional to the difference between the local concentration C and the assumed upper limit C_1. They also assumed that the root zone is unbounded, and that the constant of proportionality for root water uptake is independent of depth through the soil, resulting in the following model:

$$D\frac{dC(z)}{dz} = v(z)C(z) \quad \text{for } z > 0, \tag{1}$$

$$-\theta\frac{dv(z)}{dz} = k_0(C_1 - C(z)) \quad \text{for } z > 0, \tag{2}$$

$$C(0) = C_0, \tag{3}$$

where the salt concentration, C, and the vertical velocity of water, v, are the unknowns. The variable z denotes depth, with $z = 0$ the soil surface, and D, the diffusion coefficient, θ, the porosity, k_0, the root density, C_0, the salt concentration in sea-water, and C_1, the upper limit of salt concentration at which roots can take up water from the porous medium, are parameters.

Although their model captures interesting features of the physical problem allowing the authors to give some quantitative indications on the mechanism of soil salinization by mangroves, its mathematical simplicity does not permit to treat other relevant aspects of the problem, among them the following questions:

(A) How does evolve the salt concentration and water uptake from a given initial state towards the steady state?

(B) Is it possible that the roots zone becomes fully salinized, i.e., $C(z) = C_1$ for all z, stopping in this way the extraction of water by mangroves' roots?

(C) May gravity effects, such as fingering or convective cells, speed up the mixing of the solute in such a way that the equilibrium state is reached before the one-dimensional model prediction?

Trying to give answers to these questions, we extended the model of Passioura et al. in several ways [22, 23, 30]:

1. The physical domain.

(a) In Passioura et al. [47], the interval $\{z \in \mathbb{R} : z \geq 0\}$, with z denoting depth, was considered.

(b) In [22] the physical domain was limited to a bounded set, $\{z \in \mathbb{R} : 0 \leq z \leq H\}$, splitted in two subsets, one containing the mangrove roots and the other free of roots.

(c) In [23] we considered a three dimensional bounded domain, dropping the restriction imposed by Passioura et al. on the absence of lateral flows and on the spatial homogeneity of the root distribution. The implications of considering more spatial dimensions in the mathematical structure of the problem are important since the mass conservation equation (2) is then not sufficient to determine the field velocity, v, which is now multi-dimensional. Therefore, an additional partial differential equation must be considered to solve the problem, Darcy's law, which also forces to consider a new unknown, the pressure. However, the mathematical complications of this model have its reward since question (C) gets an answer in terms of a quantitative relationship among the parameters.

(d) In the present work, we go a step beyond by considering a three dimensional domain which is composed by two subdomains: liquid water, such as a swamp, and soil (saturated porous medium). Due to the physical differences between both media, the equations relating velocity, pressure and concentration are of different nature and new mathematical difficulties arise in their analysis.

2. The extraction function.

(a) In Passioura et al. [47], roots are supposed to fill the infinite one-dimensional domain without any vertical variation in root distribution, i.e. $k(z) = k_0$ for all $z \in (0,\infty)$. However, according to Gill [33], root distribution for mangrove species is usually shallow and extensive, often forming a dense mat of roots in the top 10 cm of the soil. Lin and Sternberg [42] measured the root distribution of a particular specie (*Rhizophora Mangle L.*) and found that the root density decreased with depth, with more than half of the fine roots being contained in the top 50 cm of the soil. Since the depth distribution of root water uptake is expected to be related to the distribution of fine roots in the soil it may be assumed that the water extraction follows the mathematical rule:

$$S(z,C) = \begin{cases} k(z)\big(1 - \dfrac{C}{C_1}\big)^r & \text{if } C \leq C_1, \\ 0 & \text{if } C > C_1, \end{cases} \tag{4}$$

where $S[\mathrm{s}^{-1}]$ is the extraction function, and the root distribution, k, is non-negative, and in accordance with [42], non-increasing with z. In addition, Passioura *et al.* [47] used the value $r = 1$ in the extraction function (4), corresponding to a linear dependence of uptake on concentration difference, which is consistent with the assumption that uptake is governed by osmotic pressure difference. However, as the authors mention, there is no experimental evidence for this choice.

(b) Therefore, in [22, 23, 30] and in this work, we considered a extraction function satisfying general functional properties, see Hypothesis H_2 in page 14. Examples like (4) for any $r > 0$ and any bounded root distribution function (e.g. non-negative and non-increasing) are included in our formulation. In particular we show that the behavior of the salinity profile differs in an essential manner between the cases $r < 1$ and $r \geq 1$ in the extraction function S, leading to an answer to question (B), again in terms of quantitative relationships among the parameters.

3. The time.

(a) In Passioura et al. [47], only the steady state problem is considered.

(b) Time dependence of the problem was considered in [22,23,30] and also in this work, giving an answer to (A). As shown in (16), the estimated values of the physical parameters imply a time scale which allows us to disregard daily variations in the salt concentration at the boundary and which yields, well within the life span of the mangroves, a steady configuration in which diffusion balances the tree-induced convection. However, the study of the time-dependent behavior of salt concentration and flow is essential for understanding how full salinization may be reached (Question (B)) and whether gravity effects shorten the time taken to salinize the soil or they do not. Therefore, both the steady state and the evolution problems are considered in this work. In particular, mathematical results on convergence of the time dependent solution to the steady state solution when $t \to \infty$ are also proven.

4. The boundary conditions.

(a) In addition to the partial differential equations, such as (1)-(2), a well-posed mathematical problem must be accomplished with boundary conditions. The situation described till now is that in which a regular inundation by tidal waters takes place giving, on average, a constant salt concentration on the surface (top boundary) of the domain, see (3). This is the most relevant and usual situation for the physical problem and it is the situation studied in [22,23,47].

(b) In [30], motivated by the occurrences observed at Ciénaga Grande de Santa Marta, Colombia, we focused in the situation in which the inflow of fresh or sea water to the mangroves domain is impeded. The continuous extraction of fresh water by the roots of mangroves drives, then, the ecosystem to a complete salinization. As reported by Botero [13] and Perdomo et al. [50], the construction of a highway along the shore in the 1950s obstructed the natural circulation of water between both parts of the road (Caribbean sea and the Ciénaga). In addition, in the 1970s, inflow of fresh water from the river Magdalena was reduced due to the construction of smaller roads and flooding control dikes. These changes caused a hypersalinization of water and soil, which resulted in approximately 70% mangrove mortality (about 360 Km^2 of mangrove forests), see [13,32]. In [30], we proposed a one-dimensional model based on laws for conservation of water and salt which lead to a system of partial differential equations with a *dynamic boundary condition* in the interface water-soil. In this chapter we continue the study of the model introducing numerical experimentation.

These extensions of the model of Passioura et al. have, as already mentioned, some implications in the mathematical analysis of the corresponding problems. The main mathematical questions we tackle are:

(i) *The existence and uniqueness of solutions of the steady state and the evolution problems.* We present the proofs of existence of solutions for two models: the water-soil model, see Section 2, and the stagnant water model, see Section 4. The water-soil model is based in a combination of the Oberbeck-Boussinesq system, and the Stokes-Darcy system, coupled with a convection-diffusion equation for the concentration. We define global unknowns in the water-soil model and split the problem into two decoupled problems: the flow problem and the concentration problem. Using well known results, see [1, 39, 40], we find solutions to these problems and, via a fixed point argument, prove the well possedness of the coupled problem, see Theorem 1 in Section 2.2. For the stagnant water problem, we use a technique based in Roth's method and consider a sequence of steady state problems satisfying a discrete dynamic boundary condition. We show that the sequence of solutions actually converges to a solution of the time-dependent problem, see Theorem 5 in Section 4.2

Regarding the uniqueness of solutions, the main difficulty is posed by the extraction function, $S(z,C)$, see (4). Whenever this function is Lipschitz continuous with respect to C, uniqueness holds. However, on the contrary, for example for $r < 1$ in (4), although we do not think that it should affect to the property of uniqueness, the proof we produced only solves the question under certain conditions, see Theorem 3 in Section 3.3. The proof is based in a duality method in which we construct suitable test functions obtained as solutions to a certain time-dependent system of partial differential equations from where the result follows. In addition to the uniqueness, our proof also includes the comparison principle for solutions which, in particular, is useful for proving the next result on asymptotic convergence.

(ii) *The convergence of the time dependent solution to the steady state solution when* $t \to \infty$. We state the results collected from previous works, see Theorems 4 and 6 in Sections 3.3 and 4.2, respectively. The proofs may be found in [22, 30].

(iii) *A stability issue* related to the formation of Bénard type cells in the multi-dimensional problem, implying a faster mixing than that predicted by the one-dimensional model. Indeed, as we already mentioned, the fresh water uptake by mangrove's roots implies a local density increase around the roots, producing the instable scenario of heavier over lighter water. Stability problems of this type have received much attention and there is abundant literature on the subject, see for instance the monographes by Straughan [56, 57] and their references. However, our stability problem is somehow unusual since the instabilities we expect to appear will attenuate and disappear when $t \to \infty$, due to the stable character of the steady state solution, in which the lower region of the domain has been filled by the heavier water.

We approach to this question from two viewpoints. First, we consider a related problem for which we may state analytical conditions under which solutions develop instabilities. To confirm that the results on the related problem are not far from our original problem, we perform several numerical experiments which demonstrate them. In addition, our experiments show that the most relevant physical parameter for stability is the permeability: low permeability soils are able to keep the instable situation of heavier over lighter water since the process becomes diffusion dominated. However, for higher permeabilities instabilities do arise and a faster mixing and approaching to the steady state takes place.

(iv) *The formation of a fully salinized region in finite time*, or *dead core*, as it is known in the field of *free boundary problems*. This property is common to all the models. Since the mathematical analysis is somehow obscure and technical, we preferred to present it for the most simple situation of one space variable, see Theorem 7 in Section 5 and [22]. We use the so called *energy method for free boundary problems*, introduced by Antontsev [2] and developed by Antontsev, Díaz and Shmarev [5]. The method roughly works as follows: first, a local energy functional given in terms of the norms of the natural energy spaces associated with the problem is introduced. Then, using the partial differential equations satisfied by the solutions (and not the boundary conditions or other non-local data) a differential inequality for such functional is obtained. Finally, the formation of a dead core is deduced from the properties of the solutions of this inequality. As we mentioned, although the method may be applied to systems of equations formulated in a very general form, we preferred to present it in the simpler one-dimensional setting of the problem, for clarity.

(v) *The discretization and numerical simulation of solutions.* The one-dimensional case is rather simple but illustrative of the behavior of solutions. We performed numerical experiments for the steady state and evolution one-dimensional models, showing the effects on the solution of the choice of a variety of data values related to the salt concentration on the top boundary (soil surface), to a dimensionless number capturing the strength of the fresh water extraction and to the power, r, on a extraction function of the type (4). The techniques employed for the discretization are based in semi-implicit finite differences schemes and Newton's method.

The discretization of the two-dimensional soil model is more subtle, see Section 3.4.1. We use a stabilized mixed finite element method in space and an implicit finite differences scheme in time. The main advantage on using a mixed formulation instead of a simpler formulation based only in concentration-pressure is that the water flow is obtained directly from the discrete solution and there is no need of deducing it by numerical differentiation of the pressure, with the loss of accuracy it implies. Since our investigation in the two-dimensional problem is centered on stability, keeping a good grade of accuracy in the flow approximation is important. Moreover, the study of the existence of solutions indicates that the decoupling of the system inherent to the mixed formulation is more natural than that of the concentration-pressure formulation in the sense that it produces energy estimates which allow to obtain a simpler proof of the existence of solutions. It is well known that classical mixed variational formulations need an adequate election of the discrete spaces for the flow and the pressure in order to satisfy the Babuska-Brezzi stability condition, see [15]. Following Masud and Huges [45], we consider a stabilized mixed finite element method for Darcy flows which allows to consider piecewise linear approximations and the same mesh for both pressure and flow.

(vi) The investigation of a one-dimensional problem in which the boundary condition is given in terms of a differential equation, i.e. a *dynamic boundary condition*. The properties studied for this model are included in (i)-(v), above. See Section 4 and [30].

2 The mathematical model: water and soil

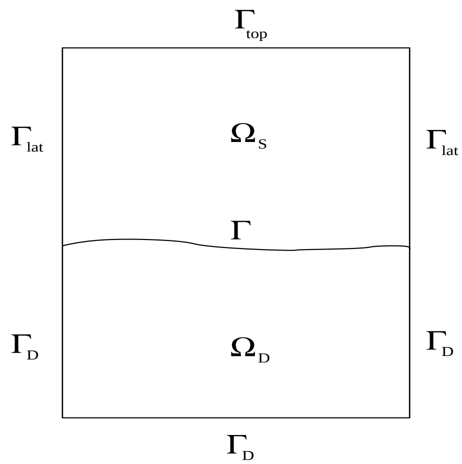

Figure 1. Water, Ω_S, and soil, Ω_D, connected through the interface Γ.

We consider the space-time domain Q_T, given as $Q_T = \Omega \times (0,T)$ for $T > 0$ an arbitrarily given final time and with the space domain $\Omega \subset \mathbb{R}^3$ which we assume, for the physical derivation of the model, to be of the cylindrical form $\Omega = B \times (-H_D, H_S)$, with H_D and H_S positive constants, and $B \subset \mathbb{R}^2$, the horizontal cross section, open and bounded.

We assume that Ω is formed by two subdomains, the water domain $\Omega_S = B \times (0, H_S)$, and, below it, the soil (water saturated porous medium) $\Omega_D = B \times (-H_D, 0)$, both connected by the interface $\Gamma = B \times \{0\}$, being therefore, $\Omega = \Omega_S \cup \Gamma \cup \Omega_D$. We use the notation $(\mathbf{x}, z)$ for points in Ω, with $\mathbf{x} \in B$ and $z \in (-H_D, H_S)$. Subscripts S and D stand for *Stokes* and *Darcy*, respectively, which are the names of the approximation equations we use in the framework of the general Oberbeck-Boussineq approximation, which reads, in the water, $\Omega_S \times (0,T)$:

$$-2\mu \,\mathbf{div}\, \mathbf{D}(\mathbf{v}_S) + \nabla p_S + \rho_S g \mathbf{e}_z = 0, \tag{5}$$

$$\operatorname{div} \mathbf{v}_S = 0, \tag{6}$$

$$\frac{\partial \rho_S}{\partial t} + \mathbf{v}_S \cdot \nabla \rho_S - D_m \Delta \rho_S = 0, \tag{7}$$

for the unknowns $\mathbf{v}_S$ $[\mathrm{m\,s^{-1}}]$, the velocity field in the water, p_S $[\mathrm{kg\,m^{-1}\,s^{-2}}]$, the hydrodynamic pressure, and ρ_S $[\mathrm{kg\,m^{-3}}]$, the density. In (5), $\mu \approx 10^{-3}\,\mathrm{kg\,m^{-1}\,s^{-1}}$ is the water dynamic viscosity coefficient, $g \approx 10\,\mathrm{m\,s^{-2}}$ is the modulus of the gravity acceleration and $\mathbf{e}_z$ is the vertical vector pointing upwards. Observe that, for constant viscosity, the deformation rate tensor

$$\mathbf{D}(\mathbf{v}_S) = \frac{1}{2}(\nabla \mathbf{v}_S + (\nabla \mathbf{v}_S)^T),$$

Table 1. Some typical parameter values

Parameter	Symbol	S.I.
Water density	ρ_0	$1000\ \mathrm{kg\,m^{-3}}$
Salt density	ρ_{salt}	$2170\ \mathrm{kg\,m^{-3}}$
Threshold salt density for mangrove water uptake	ρ_{max}	$1070\ \mathrm{kg\,m^{-3}}$
Dynamic viscosity	μ	$10^{-3}\ \mathrm{kg\,m^{-1}\,s^{-1}}$
NaCl molecular diffusion in water	D_m	$10^{-9}\ \mathrm{m^2\,s^{-1}}$
Porosity	θ	0.5
Permeability	κ	$10^{-11} - 10^{-13}\ \mathrm{m^2}$
Hydraulic conductivity	K	$7\times 10^5[\kappa]^1\ \ \mathrm{m\,s^{-1}}$
Mangroves' transpiration rate	τ_0	$10^{-8} - 10^{-7}\ \mathrm{m\,s^{-1}}$

is such that $2\mu\,\mathbf{div}(\mathbf{D}(\mathbf{v}_S)) = \mu\Delta\mathbf{v}_S$. The water and salt solution density is given as $\rho_S = \rho(c_S)$, with

$$\rho(c) = (1-c)\rho_0 + c\rho_s, \tag{8}$$

with c_S the salt concentration in percentage points, ρ_0 a reference density, e.g., water density in standard conditions, $\rho_0 \approx 1000\,\mathrm{kg\,m^{-3}}$, and $\rho_s \approx 2170\,\mathrm{kg\,m^{-3}}$, the salt density. We note that salt concentration in sea water is $c_{sea} \approx 3\%$, well below than saturation concentration $c_{sat} \approx 25\%$. Moreover, the maximum salt concentration that mangroves may tolerate is $c_{max} \approx 6\%$, always far away from the saturation level. The positive constant D_m is the molecular diffusion of NaCl in water. Different authors give different (but close) values for it, ranging from $D_m = 1.5\times 10^{-9}\ \mathrm{m^2\,s^{-1}}$, see [47] to $D_m = 0.75\times 10^{-9}\ \mathrm{m^2\,s^{-1}}$, see [34]. In the simulations, we take the intermediate value $D_m \approx 10^{-9}\,\mathrm{m^2\,s^{-1}}$. See Table 1 for references on standard values of physical parameters.

Regarding the soil subdomain, we consider the case where the mangroves roots are present within an homogeneous porous medium located below Γ. This porous medium is characterized by a constant porosity $\theta \approx 0.5$, indicating that we are assuming the mangroves roots to be homogenized throughout the porous medium, without affecting its properties. Assuming, as usual, that the fluid flow is governed by Darcy's law and disregarding density variations in the mass balance equation of the fluid we find the following system of equations in the porous medium, $\Omega_D \times (0,T)$:

$$\mathbf{v}_D + \frac{\kappa}{\mu}(\nabla p_D + \rho_D g \mathbf{e}_z) = 0, \tag{9}$$

$$\operatorname{div}\mathbf{v}_D + S(\cdot,\rho_D) = 0, \tag{10}$$

$$\theta\frac{\partial\rho_D}{\partial t} + \operatorname{div}((\rho_D-\rho_0)\mathbf{v}_D - \theta\mathbf{D}\nabla\rho_D) = 0, \tag{11}$$

for the unknowns $\mathbf{v}_D$, the velocity field in the porous medium, p_D, the pressure, and $\rho_D = \rho(c_D)$, the density of the solute. Parameter κ is the permeability, a measure of the ability of the porous medium to conduct the fluid, which plays a crucial role in the stability of the system. The range of values of interest is from $\kappa \approx 10^{-11}\ \mathrm{m^2}$, corresponding to well

[1] $[\ \cdot\ ]$ denotes a dimensionless value.

sorted sand, sand and gravel or peat, to $\kappa \approx 10^{-13}$ m^2 corresponding to very fine sand, silt or layered clay. The hydrodynamic dispersion tensor $\mathbf{D}$ [m^2 s^{-1}] is assumed to be constant and isotropic, and of the form see [31], $\mathbf{D} = D\mathbf{I}$, with $D = D_m + D_d$, D_d the hydrodynamic dispersion coefficient and $\mathbf{I}$ the identity matrix. For small Péclet numbers, as in our mangroves problem, D_m and D_d are of similar order of magnitude [31], and so is D, implying that diffusive processes in water and in the porous medium have a similar time scale .

The *extraction* function S [s^{-1}] is a function satisfying general conditions which will be described later, see page 14. A typical example we will keep on mind is given by

$$S(\mathbf{x},z,\rho) = \begin{cases} k(z)\big(1 - \dfrac{\rho-\rho_0}{\rho_{max}-\rho_0}\big)^r & \text{for } \rho_0 \le \rho \le \rho_{max}, \\ 0 & \text{for } \rho > \rho_{max}, \end{cases} \tag{12}$$

with $r > 0$, $\rho_{max} = \rho(c_{max})$ and $c_{max} \approx 6\%$ the maximum salt concentration at which mangroves may uptake fresh water. The *root distribution function* k [s^{-1}] satisfies

$$\int_{\Omega_D} k(z)d\mathbf{x}dz = |B| \int_{-H_D}^{0} k(z)dz = k_0,$$

being k_0 [m^3 s^{-1}] the total amount of root water uptake with no salt present, related to the corresponding mangrove transpiration rate, τ_0, by $\tau_0 = k_0/|B|$ [m s^{-1}]. Observe that $k(z)$ represents a root distribution homogeneous in the horizontal plane, while the density dependent term in (12) is a switch mechanism, which stops the roots water uptake when the threshold salt concentration is attained in a particular zone. We often consider the following example as root distribution function: let $H_{root} \in (0, H_D)$ denote the depth of the roots region. We set

$$k(z) = \begin{cases} \dfrac{\tau_0}{H_{root}} & \text{for } z \in (-H_{root}, 0), \\ 0 & \text{for } z \in (-H_D, -H_{root}). \end{cases} \tag{13}$$

Remark 1 System (9)-(11) has two equilibrium states for constant density. Indeed, assume ρ_D is constant. Combining equations (10) and (11) we obtain

$$(\rho_D - \rho_0)S(\cdot, \rho_D) = 0,$$

which, according to definition (12), only has the solutions: (i) $\rho_D = \rho_0$, and (ii) $\rho_D = \rho_{max}$. These states correspond to trivial situations in which no dynamic is generated due to: (i) no salt present in the water, and (ii) the threshold level of salt concentration at which mangroves may uptake water is reached.

2.1 Dimensionless formulation

The main clues for the rescaling are the characteristics scales of space and velocity in the porous medium domain, where the dynamics of the problem has its origin. A characteristic velocity in Ω_D is given either by the hydraulic conductivity, $K \approx 10^{-6} - 10^{-8}$ m s^{-1} or by the slower mangroves transpiration rate, $\tau_0 \approx 10^{-8}$ m s^{-1}. We choose the former,

$$\tilde{\mathbf{v}}_D = \frac{1}{K}\mathbf{v}_D, \quad \text{with} \quad K = \frac{\kappa(\rho_{max} - \rho_0)g}{\mu}. \tag{14}$$

The characteristic length in the porous medium may be chosen as that of the mangrove roots maximum depth, or the depth of the phreatic layer, both in the oder of meters. We take

$$\tilde{\mathbf{x}} = \frac{\mathbf{x}}{H}, \quad \tilde{z} = \frac{z}{H}, \quad \text{with } H = H_D \approx 1\,\mathrm{m}. \tag{15}$$

The corresponding characteristic time is, therefore, given by $H/K \approx 10^7$ s, which is very short for our pourposes. Another natural characteristic time, more suitable than the previous, is that implied by the diffusion processes in which we are interested, which may be taken as

$$\tilde{t} = \frac{D}{H^2}t, \tag{16}$$

which is in the order of tenths of years. The rest of unknowns in Ω_D are fixed as follows:

$$\tilde{p}_D = \frac{p_D - \rho_0 gHz}{(\rho_{max} - \rho_0)gH}, \quad u_D = \frac{\rho(c_D) - \rho_0}{\rho_{max} - \rho_0}, \tag{17}$$

and $\tilde{f}(\tilde{\mathbf{x}}, \tilde{z}, u_D) = S(H\tilde{\mathbf{x}}, H\tilde{z}, (\rho_{max} - \rho_0)u_D + \rho_0)$. Setting $\tilde{T} = TD/H^2$ and $\tilde{\Omega}_D = \frac{1}{H}\Omega_D$ equations (9)-(11) transform to (omitting tildes)

$$\mathbf{v}_D + \nabla p_D + u_D \mathbf{e}_z = 0, \tag{18}$$

$$\operatorname{div} \mathbf{v}_D + mf(\cdot, u_D) = 0, \tag{19}$$

$$\frac{\partial u_D}{\partial t} + R\,\mathbf{div}(u_D \mathbf{v}_D) - \Delta u_D = 0, \tag{20}$$

in $\Omega_D \times (0,T)$, with

$$R = \frac{KH}{\theta D}, \quad m = \frac{k_0}{KH^2} \approx \frac{\tau_0}{K}. \tag{21}$$

R is a Rayleigh number while m is a dimensionless number expressing the strength of the extraction process. Observe that the example for f given by (12) takes the dimensionless form

$$f(\mathbf{x}, z, u_D) = k(z)(1 - u_D)_+^r \tag{22}$$

with, for $d = H_{root}/H \in (0,1)$,

$$k(z) = \begin{cases} 1/d & \text{if } z \in [0,d], \\ 0 & \text{if } z \in (d,1]. \end{cases} \tag{23}$$

The dimensionless analysis in the water domain is more subtle. If there is no extraction and the water density, ρ_S, keeps constant then the solution is given by $\mathbf{v}_S = const.$ and $\nabla p_S = -\rho_S \mathbf{e}_z$. When the extraction starts and the flow of more saline water enters from the porous medium to the water, the situation in the water is nearly stable since the more saline water tends to stay at the bottom of Ω_S. Therefore, the length scale in Ω_S is shorter than in Ω_D, no matter the actual height of the water column. The possible (and weak) dynamical effects on the water are mainly restricted to a thin layer over the interface. Taking $\tilde{\mathbf{v}}_S = \frac{\theta}{K}\mathbf{v}_S$ and a similar rescaling for $\tilde{p}_S$ and u_S than in (17), we obtain (omitting tildes)

$$-2\nu\,\mathbf{div}\,\mathbf{D}(\mathbf{v}_S) + \nabla p_S + u_S\mathbf{e}_z = 0, \tag{24}$$

$$\operatorname{div}\mathbf{v}_S = 0, \tag{25}$$

$$\frac{\partial u_S}{\partial t} + R\mathbf{v}_S \cdot \nabla u_S - \Delta u_S = 0, \tag{26}$$

in $\Omega_S \times (0,T)$, with $\nu = \theta\kappa/H^2$. For typical physical values of the system parameters, see Table 1, we have

$$R \approx 10^2 - 10^4, \quad m \approx 10^{-3} - 1, \quad \nu \approx 10^{-12}. \tag{27}$$

It is clear that the order of magnitude of the coefficient ν of the *viscous* term is very small when compared with the other terms. However, from the mathematical point of view, if the water domain is to be taken into account, the viscous term is necessary for the well possedness of the problem. In Section 3 we neglect the water domain and study the problem only in the porous medium.

Auxiliary conditions: The boundary conditions depend on the particular physical situation we want to model. For simplicity, we think in a spatial domain which is isolated from horizontal and upward fluxes. This translates onto, for $h = H_S/H_D$,

$$\mathbf{v}_S = 0 \quad \text{and} \quad \nabla u_S \cdot \mathbf{n}_S = 0 \quad \text{on } \partial B \times (0,h) \times (0,T), \tag{28}$$

$$\mathbf{v}_D \cdot \mathbf{n}_D = \nabla u_D \cdot \mathbf{n}_D = 0 \quad \text{on } \partial B \times (-1,0) \times (0,T). \tag{29}$$

$$\mathbf{v}_D \cdot \mathbf{n}_D = \nabla u_D \cdot \mathbf{n}_D = 0 \quad \text{on } B \times \{-1\} \times (0,T), \tag{30}$$

with $\mathbf{n}_S$ and $\mathbf{n}_D$ the outward unit normal vectors to Ω_S and Ω_D, respectively.

In the top boundary, $\Gamma_{top} = B \times \{h\}$, the situation is more complicated. Due to the extraction term in (19), a continuous extraction of water takes place in the porous medium, Ω_D, which must be either compensated by a decrease of the water level in Ω_S either by an inflow of the same quantity of water through the top boundary. First alternative implies the consideration of a variable water domain while second possibility translates to the following compatibility condition

$$\int_{\Gamma_{top}} \mathbf{v}_S \cdot \mathbf{n} = -m \int_{\Omega_D} f(\cdot, u_D) \quad \text{for a.e. } t \in (0,T). \tag{31}$$

Since both alternatives add important mathematical difficulties to the problem, a first simplifying step is to consider that the volume of water extracted by the mangroves roots from Ω_D is small when compared to the total volume of water in Ω_S, allowing us to assume that neither the boundary of this domain moves nor the water volume changes (significatively). Then, ignoring the compatibility condition (31), we assume

$$\mathbf{v}_S = 0 \quad \text{and} \quad u_S = u_{top} \quad \text{on} \quad \Gamma_{top} \times (0,T), \tag{32}$$

with $u_{top} = (\rho(c_{top}) - \rho_0)/(\rho_{max} - \rho_0)$ prescribing the salt concentration in the top boundary, which normally results from a mixture of sea and fresh water.

The transmission conditions on the interface Γ is a very subtle question which has been object of intense investigation, see Beavers and Joseph [9] and Saffman [52] for pioneering works or Jäger and Mićelik [36], for a more recent discussion. Following the current trend, we set them in the following way:

- Mass conservation:

$$\mathbf{v}_S \cdot \mathbf{n}_S + \mathbf{v}_D \cdot \mathbf{n}_D = 0. \tag{33}$$

- Balance of normal forces:

$$p_S - 2\nu \mathbf{n}_S \cdot \mathbf{D}(\mathbf{v}_S) \cdot \mathbf{n}_S = p_D. \tag{34}$$

- Beavers-Joseph-Saffman condition:

$$\mathbf{v}_S \cdot \tau_j = -2\frac{\sqrt{\kappa}}{\alpha} \mathbf{n}_S \cdot \mathbf{D}(\mathbf{v}_S) \cdot \tau_j, \tag{35}$$

with τ_j, $j = 1,2$ an orthogonal system of tangent vectors on Γ, κ the porous medium permeability and $\alpha > 0$ an experimentally determined dimensionless parameter.

- Continuity for concentration and normal component of concentration flow:

$$u_S = u_D \quad \text{and} \quad \nabla u_S \cdot \mathbf{n}_S + \nabla u_D \cdot \mathbf{n}_D = 0. \tag{36}$$

We , finally, prescribe initial conditions:

$$\mathbf{v}_S(\cdot,0) = \mathbf{v}_0 \quad \text{and} \quad u_S(\cdot,0) = u_{S,0} \quad \text{on } \Omega_S, \tag{37}$$

$$u_D(\cdot,0) = u_{D,0} \quad \text{on } \Omega_D. \tag{38}$$

with $u_{S,0} = (\rho(c_{S,0}) - \rho_0)/(\rho_{max} - \rho_0)$ and $u_{D,0} = (\rho(c_{D,0}) - \rho_0)/(\rho_{max} - \rho_0)$.

Although for the deduction of some properties such as stability, or for the numerical simulations we will keep the present approach, we may generalize our assumptions on the set Ω and the function f for the proof of existence of solutions and other qualitative results. The main property function f should satisfy, apart from regularity requirements, is to *switch off* the dynamics of the system (water extraction by mangroves roots) when the solute concentration, u_D, reaches the threshold value $u_D = 1$.

Hypothesis and definitions

H_1. The spatial domain $\Omega \subset \mathbb{R}^n$ is bounded and decomposed in two subdomains, Ω_S and Ω_D, such that $\Omega_S \cap \Omega_D = \emptyset$ and $\bar{\Omega}_S \cap \bar{\Omega}_D = \bar{\Gamma}$, for an open set $\Gamma \subset \mathbb{R}^{n-1}$, implying $\Omega = \Omega_S \cup \Omega_D \cup \Gamma$. The boundary of Ω, $\partial\Omega$, is Lipschitz continuous and decomposed as $\Gamma_S = (\partial\Omega \cap \partial\Omega_S)/\Gamma$ and $\Gamma_D = (\partial\Omega \cap \partial\Omega_D)/\Gamma$. We further assume that $\Gamma_S = \Gamma_{top} \cup \Gamma_{lat}$, with $\Gamma_{top} \cap \Gamma_{lat} = \emptyset$ and with Γ_{top} of positive $n-1$ dimensional measure.

H_2. The function $f : \bar{\Omega}_D \times [0,1] \to \mathbb{R}$ satisfies

$$f(\mathbf{x},\cdot) \in C([0,1]) \text{ for a.e. } \mathbf{x} \in \Omega_D,$$
$$f(\cdot,s) \in L^\infty(\Omega_D) \text{ for all } s \in [0,1],$$
$$f(\mathbf{x},\cdot) \text{ is non-increasing in } [0,1] \text{ and } f(\mathbf{x},1) = 0 \text{ for a.e. } \mathbf{x} \in \Omega_D.$$

Note that, in particular, $f \geq 0$ in $\bar{\Omega}_D \times [0,1]$.

H_3. The initial and boundary data posses the regularity

$$u_0 \in L^\infty(\Omega) \quad \text{and} \quad 0 \leq u_0 \leq 1 \quad \text{a.e. in } \Omega,$$
$$u_{top} \in H^1(0,T;L^2(\Omega)) \cap L^2(0,T;H^1(\Omega)) \quad \text{and} \quad 0 \leq u_{top} \leq 1 \quad \text{a.e. in } Q_T.$$

H_4. The numbers ν, R and m are positive.

The boundary conditions (28)-(32) are redefined as

$$\mathbf{v}_S = 0 \quad \text{on } \Gamma_S \times (0,T), \tag{39}$$
$$u_S = u_{top} \quad \text{on } \Gamma_{top} \times (0,T), \tag{40}$$
$$\nabla u_S \cdot \mathbf{n}_S = 0 \quad \text{on } \Gamma_{lat} \times (0,T), \tag{41}$$
$$\mathbf{v}_D \cdot \mathbf{n}_D = \nabla u_D \cdot \mathbf{n}_D = 0 \quad \text{on } \Gamma_D \times (0,T). \tag{42}$$

The problem under study is formed by the systems of equations in the water, (24)-(26), and in the soil (18)-(20), together with the boundary conditions (39)-(42), the transmission conditions (33)-(36) and the initial data (37) and (38). We shall refer to this problem as to **Problem P**.

2.2 Existence of solutions

In this section we provied the usual functional setting for developing a suitable notion of weak solution for Problem P. For constant concentration, the resulting mathematical model, known as the Stokes-Darcy model, has been recently but widely treated in the literature. See [9,36,48] for pioneering work on the subject and Layton, Schieweck and Yotov [40] as a fundamental reference for the results in this section.

The treatment of variable concentration is more recent and different approaches and formulations has been introduced to deal with it, normally motivated either by the mathematical difficulties inherent to the numerical discretization, either by the diversity of situations the model apply to. Since our aim here is proving the well possedness of the problem, we do not need to dive into the mathematical subtleties of the numerical analysis and therefore, may give a rather simple proof. Observe that for our application, the water domain is not specially significant since the dynamics of the problem is originated in the subsurface and the consequences of such dynamics do not affect substantially to the water domain. Indeed, the salinization of the soil is a stable situation in the water region since heavier water tends to stay at the bottom and only moves at the low velocities induced by diffusion. The most remarkable effect when considering the water above the soil is related to physical situations in which the water is trapped in its domain (no water inflow into the water region) causing a slow but progressive salinization of the full system water-soil, see Section 4. However, we feel that showing the well possedness of the entire water-soil model for general conditions is a good starting point for latter particularization.

We will prove the existence of solutions of Problem P as globally defined functions in Ω. We start by considering two problems which result from uncoupling concentration and flow equations and, once that we prove the well possedness of these problems and we find suitable estimates on their solutions, we apply the Shauder's fixed point theorem to an operator which couples both problems and provides a solution of the original problem.

Let us introduce the flow space

$$H_0(\mathrm{div},\Omega)=\left\{\phi\in L^2(\Omega)^n:\mathrm{div}\,\phi\in L^2(\Omega)\quad\text{and}\quad\phi\cdot\mathbf{n}=0\text{ on }\partial\Omega\right\},$$

with norm

$$\|\phi\|_{H_0(\mathrm{div},\Omega)}=(\|\phi\|^2_{L^2(\Omega)}+\|\,\mathrm{div}\,\phi\|^2_{L^2(\Omega)})^{1/2},$$

and consider the subspace $\mathcal{W}_T\subset L^2(0,T;H_0(\mathrm{div},\Omega))$ of divergence bounded vectors

$$\mathcal{W}_T=\left\{\phi\in L^2(0,T;L^2(\Omega)^n):\mathrm{div}\,\phi\in L^\infty(Q_T)\right\}$$

with norm

$$\|\phi\|_{\mathcal{W}_T}=(\|\phi\|^2_{L^2(Q_T)}+\|\,\mathrm{div}\,\phi\|^2_{L^\infty(Q_T)})^{1/2}.$$

The concentration problem: Let $\tilde{\mathbf{v}}\in L^2(0,T;H_0(\mathrm{div},\Omega))\cap\mathcal{W}_T$ be given and set $u=(u_S,u_D)$. The problem is to find $u:\bar{Q}_T\to\mathbb{R}$ such that

$$\frac{\partial u}{\partial t}+R\,\mathbf{div}(u\tilde{\mathbf{v}})-\Delta u=0\quad\text{in }Q_T,\tag{43}$$

$$u=u_{top}\quad\text{on }\Gamma_{top}\times(0,T),\tag{44}$$

$$\nabla u\cdot\mathbf{n}=0\quad\text{on }\Gamma_N\times(0,T),\tag{45}$$

$$u(\cdot,0)=u_0\quad\text{on }\Omega,\tag{46}$$

with $\Gamma_N=\partial\Omega/\bar{\Gamma}_{top}$.

The flow problem: We follow the approach of [40]. We start with the formulation splitted in water and porous medium domains. Let $\tilde{u}\in L^2(Q_T)$ be given and set $\tilde{u}_S=\tilde{u}|_S\in L^2(0,T;\Omega_S)$ and $\tilde{u}_D=\tilde{u}|_D\in L^2(0,T;\Omega_D)$. Find $\mathbf{v}_S:\bar{\Omega}_S\times[0,T]\to\mathbb{R}^n$, $p_S:\bar{\Omega}_S\times[0,T]\to\mathbb{R}$, $\mathbf{v}_D:\bar{\Omega}_D\times[0,T]\to\mathbb{R}^d$ and $p_D:\bar{\Omega}_D\times[0,T]\to\mathbb{R}$ such that, for a.e. $t\in(0,T)$,

$$-2\nu\,\mathbf{div}\,\mathbf{D}(\mathbf{v}_S)+\nabla p_S=-\tilde{u}_S\mathbf{e}_z\quad\text{in }\Omega_S,\tag{47}$$

$$\mathrm{div}\,\mathbf{v}_S=0\quad\text{in }\Omega_S,\tag{48}$$

$$\mathbf{v}_S=0\quad\text{on }\Gamma_S,\tag{49}$$

and

$$\mathbf{v}_D+\nabla p_D=-\tilde{u}_D\mathbf{e}_z\quad\text{in }\Omega_D,\tag{50}$$

$$\mathrm{div}\,\mathbf{v}_D=-mf(\cdot,\tilde{u}_D)\quad\text{in }\Omega_D,\tag{51}$$

$$\mathbf{v}_D\cdot\mathbf{n}_D=0\quad\text{on }\Gamma_D,\tag{52}$$

together with the transmission conditions on the interface Γ given by (33)-(35).

Despite this two-domains formulation of the flow problem, a weak global formulation may be defined and proved to be well-posed, see [40]. On the other hand, the existence and uniqueness of weak solutions of the concentration problem is also a well known issue, see [1, 39]. We may therefore define the operator

$$S:L^2(Q_T)\to L^2(Q_T),\quad S(\tilde{u})=u,\tag{53}$$

where u is the weak solution of the concentration problem, (43)-(46), corresponding to $\tilde{\mathbf{v}} = \mathbf{v}$, being $\mathbf{v} = (\mathbf{v}_S, \mathbf{v}_D)$ the global weak solution of the flow problem, (47)-(52), corresponding to $\tilde{u}$. Clearly, a fixed point of S is a solution of the whole Problem P.

Before proving the existence of such fixed point we give suitable estimates of the solutions of the uncoupled problems. For defining the flow problem (47)-(52) globally in Ω we need to introduce some functional tools. We start by defining, for all $s \in [0,1]$

$$F(\mathbf{x},s) = \begin{cases} 0 & \text{if } \mathbf{x} \in \Omega_S, \\ mf(\mathbf{x},s) & \text{if } \mathbf{x} \in \Omega_D. \end{cases} \tag{54}$$

Following [40], let

$$X_S = \left\{ \phi_S \in H^1(\Omega_S)^n : \phi_S = 0 \text{ on } \Gamma_S \right\}, \tag{55}$$

equipped with the norm

$$\|\phi_S\|_{X_S} = \|\nabla \phi_S\|_{L^2(\Omega)^n},$$

and $M_S = L^2(\Omega_S)$, denote the usual velocity-pressure spaces on Ω_S. The velocity space X_D on Ω_D is the subspace of

$$H(\text{div};\Omega_D) = \left\{ \phi_D \in L^2(\Omega)^n : \text{div}\, \phi_S \in L^2(\Omega) \right\} \tag{56}$$

consisting on functions with zero normal trace on Γ_D and equipped with the norm

$$\|\phi_D\|_{H(\text{div};\Omega_D)} = (\|\phi_D\|^2_{L^2(\Omega_D)^n} + \|\text{div}\, \phi_D\|^2_{L^2(\Omega_D)})^{1/2}.$$

Since the restriction of $\phi_D \cdot \mathbf{n}_D$ may not lie in $H^{-1/2}(\Gamma_D)$, we define [58]

$$X_D = \left\{ \phi_D \in H(\text{div};\Omega_D) : \langle \phi_D \cdot \mathbf{n}_D, w \rangle_{\Gamma_D} = 0 \text{ for all } w \in H^1_{0,\Gamma}(\Omega_D) \right\},$$

where $\langle \cdot,\cdot \rangle_B$ denotes scalar product in $L^2(B)$ and

$$H^1_{0,\Gamma}(\Omega_D) = \left\{ w \in H^1(\Omega_D) : w = 0 \text{ on } \Gamma \right\}.$$

The pressure space is, as usual, $M_D = L^2(\Omega_D)$. Defining $X = X_S \times X_D$, we represent $\phi \in X$ as $\phi = (\phi_S, \phi_D)$, with $\phi_S \in X_S$ and $\phi_D \in X_D$. The norm on X is, then

$$\|\phi\|_X = (\|\phi_S\|^2_{X_S} + \|\phi_D\|^2_{X_D})^{1/2}.$$

Similarly, we define M as

$$M = \{ q = (q_S, q_D) \in M_S \times M_D : \langle q_S, 1 \rangle_{\Omega_S} + \langle q_D, 1 \rangle_{\Omega_D} = 0 \},$$

with norm

$$\|q\|_M = (\|q_S\|^2_{L^2(\Omega_S)} + \|q_D\|^2_{L^2(\Omega_D)})^{1/2}.$$

The procedure to deduce a weak formulation for the flow problem is as usual, multiplying the equations of the strong formulation (47)-(52) by test functions, integrating by parts, using the boundary and interface conditions and adding the resulting identities. In order to write down these identities, we begin by defining the following bilinear forms for the global functions $\mathbf{v} = (\mathbf{v}_S, \mathbf{v}_D)$, $\phi = (\phi_S, \phi_D)$, etc.,

$$a(\mathbf{v},\phi) = \nu\langle \nabla \mathbf{v}_S, \nabla \phi_S\rangle_{\Omega_S} + \langle \mathbf{v}_D, \phi_D\rangle_{\Omega_D} + \frac{\nu\alpha}{\sqrt{\kappa}}\sum_{j=1}^{n-1}\langle \mathbf{v}_S\cdot\tau_j, \phi\cdot\tau_j\rangle_\Gamma, \tag{57}$$

$$b(\phi,q) = -\langle q_S, \operatorname{div}\phi_S\rangle_{\Omega_S} - \langle q_D, \operatorname{div}\phi_D\rangle_{\Omega_D}. \tag{58}$$

Observe that the third term at the right hand side of (57) captures the Beavers-Joseph-Saffman condition. The other transmission conditions manifests through the flux continuity condition (33) and the definition of the Lagrange multiplier, λ, given by

$$p_S - 2\nu\mathbf{n}_S\cdot\mathbf{D}(\mathbf{v}_S)\cdot\mathbf{n}_S = \lambda = p_D \quad \text{on} \quad \Gamma. \tag{59}$$

Indeed, the following interface term appears after the integration by parts

$$\int_\Gamma (p_S - 2\nu\mathbf{n}_S\cdot\mathbf{D}(\mathbf{v}_S)\cdot\mathbf{n}_S)\phi_S\cdot\mathbf{n}_S + \int_\Gamma p_D\phi_D\cdot\mathbf{n}_D. \tag{60}$$

Using (59) in (60) we get

$$\int_\Gamma \lambda(\phi_S\cdot\mathbf{n}_S + \phi_D\cdot\mathbf{n}_D), \tag{61}$$

which we want to vanish for $\phi = \mathbf{v}$, due to the flux continuity condition (33). Instead of adding this term into the set of equations to solve, we incorporate it to the space of admissible functions for being solutions of our problem. The task here is to select an appropriate space for the bilinear form (61), or written in another way,

$$b_I(\phi,\mu) = \langle \phi_S\cdot\mathbf{n}_S + \phi_D\cdot\mathbf{n}_D, \lambda\rangle_\Gamma, \tag{62}$$

to be continuous in $X\times\Lambda$, for some functional space, Λ, of Langrange multipliers defined on Γ. It is proved in [40] that a satisfactory choice is $\Lambda = H^1_{00}(\Gamma)$ (a subspace of $L^2(\Gamma)$, see [44]). With this choice, the space of functions of X satisfying the flux continuity condition (33) given by

$$V = \left\{\phi\in X : b_I(\phi,\mu) = 0 \text{ for all } \mu\in H^1_{00}(\Gamma)\right\}, \tag{63}$$

is a closed subspace of X, from whose inherits the norm. Other properties of this formulation are proved in [40], leading to the following result.

Lemma 1 *For any $\tilde u\in L^2(Q_T)$ there exists a unique weak solution $(\mathbf{v},p)\in L^2(0,T;V)\times L^2(0,T;M)$ of the flow problem, defined as*

$$\begin{cases} a(\mathbf{v},\phi) + b(\phi,p) = -\langle \tilde u\mathbf{e}_z, \phi\rangle_\Omega & \text{for all } \phi\in V, \\ b(\mathbf{v},q) = -\langle F(\cdot,\tilde u), q\rangle_\Omega & \text{for all } q\in M, \end{cases} \tag{64}$$

for a.e. $t\in(0,T)$. In addition $\mathbf{v}\in\mathcal{W}_T$, $\|\mathbf{v}\|_{\mathcal{W}_T}\le c$, and the norms

$$\|\mathbf{v}\|_{L^2(0,T;X)}, \qquad \|p\|_{L^2(Q_T)} \tag{65}$$

are bounded by $c(\|\tilde u\|_{L^2(Q_T)}+1)$, with c independent of $\tilde u$.

Proof. The proof of existence and uniqueness of solutions is a direct consequence of Theorem 3.1 of [40]. We now prove the uniform estimates. Let $(\mathbf{v},p)\in L^2(0,T;V)\times L^2(0,T;M)$ be the solution of problem (64) and let c denote a generic constant independent of $\tilde{u}$ whose value may change along the proof. As in Lemma 3.2 of [40], we may construct a test function $\phi\in V$ such that, for a.e. $t\in(0,T)$

$$\operatorname{div}\phi = p \quad \text{in } \Omega, \quad \phi = 0 \quad \text{on } \partial\Omega, \quad \text{and } \|\phi\|_X \leq c\|p\|_M. \tag{66}$$

Using this test function in the second equation of (64) we get

$$\|p\|^2_{L^2(\Omega)} = b(\phi,p) = -a(\mathbf{v},\phi) - \langle \tilde{u}\mathbf{e}_z,\phi\rangle_\Omega \leq c_1\|\mathbf{v}\|_X\|\phi\|_X + \|\tilde{u}\|_{L^2(\Omega)}\|\phi\|_{L^2(\Omega)}. \tag{67}$$

Poincare's inequality and the estimate in (66) give

$$\|p\|_{L^2(\Omega)} \leq c\big(\|\mathbf{v}\|_X + \|\tilde{u}\|_{L^2(\Omega)}\big). \tag{68}$$

Lemma 2.2 of [40] implies that $\operatorname{div}\mathbf{v}\in L^2(Q_T)$ and the second equation of (64) implies that $\operatorname{div}\mathbf{v} = c + F(\cdot,\tilde{u})$ a.e. in Q_T. Therefore, due to Hypothesis H_2 on the boundedness of f we get

$$\|\operatorname{div}\mathbf{v}\|_{L^\infty(\Omega)} \leq c, \tag{69}$$

and hence $\|\mathbf{v}\|_{\mathcal{W}_T}\leq c$. On the other hand, using $\mathbf{v}$ as test function in the first equation of (64), we obtain

$$a(\mathbf{v},\mathbf{v}) = -\langle \tilde{u}\mathbf{e}_z,\mathbf{v}\rangle_\Omega + \langle F(\cdot,\tilde{u}),p\rangle_\Omega \leq \|\tilde{u}\|_{L^2(\Omega)}\|\mathbf{v}\|_{L^2(\Omega)} + c\|\tilde{u}\|_{L^2(\Omega)}\|p\|_{L^2(\Omega)}, \tag{70}$$

where we used Hypothesis H_2. Poincare's inequality and (68) imply

$$a(\mathbf{v},\mathbf{v}) \leq c\|\tilde{u}\|_{L^2(\Omega)}(\|\mathbf{v}\|_X + \|\tilde{u}\|_{L^2(\Omega)}). \tag{71}$$

Finally, since $\|\mathbf{v}\|^2_X \leq (a(\mathbf{v},\mathbf{v}) + \|\operatorname{div}\mathbf{v}\|^2_{L^2})^{1/2}$, we deduce (65) from a combination of (68), (69) and (71), Young's inequality and integration in $(0,T)$. $\square$

For the concentration problem, we consider the closed subspace of $H^1(\Omega)$ given by

$$\mathcal{V} = \left\{\varphi\in H^1(\Omega) : \varphi = 0 \text{ on } \Gamma_{top}\right\},$$

and equipped with the norm $\|v\|_{\mathcal{V}} = \|\nabla v\|_{L^2(\Omega)}$.

Lemma 2 *For any $\tilde{\mathbf{v}}\in L^2(0,T;H_0(\operatorname{div},\Omega))\cap\mathcal{W}_T$ there exists a unique weak solution, u, of the concentration problem (43)-(46), defined as*

$$\begin{aligned}
&u\in u_{top} + L^2(0,T;\mathcal{V})\cap H^1(0,T;\mathcal{V}')\cap L^\infty(Q_T)\\
&< u_t,\varphi > + R\int_\Omega \varphi\tilde{\mathbf{v}}\cdot\nabla u + \int_\Omega \nabla u\cdot\nabla\varphi = \int_\Omega uF(\cdot,u)\varphi,\\
&\lim_{t\to 0}\|u(\cdot,t) - u_0\|_{L^2(\Omega)} = 0,
\end{aligned} \tag{72}$$

for all $\varphi\in\mathcal{V}\cap L^\infty(\Omega)$ and for a.e. $t\in(0,T)$. In addition, the norms

$$\|u\|_{L^\infty(Q_T)}, \quad \|u\|_{L^2(0,T;\mathcal{V})}, \quad \|u_t\|_{L^2(0,T;\mathcal{V}')},$$

are bounded in terms of the norms $\|u_0\|_{L^\infty(\Omega)}$, $\|\tilde{\mathbf{v}}\|_{L^2(0,T;H_0(\operatorname{div},\Omega))\cap\mathcal{W}_T}$, and

$$\|u_{top}\|_{H^1(0,T;L^2(\Omega))\cap L^2(0,T;H^1(\Omega))\cap L^\infty(Q_T)}.$$

Finally, it holds

$$\min\{u_{top},u_0\} \leq u \leq 1 \quad \text{a.e. in } Q_T.$$

Proof. We consider a sequence $\{\tilde{\mathbf{v}}_n\} \subset L^\infty(0,T;L^\infty(\Omega)^d) \cap L^2(0,T;X) \cap \mathcal{W}_T$ such that

$$\tilde{\mathbf{v}}_n \to \tilde{\mathbf{v}} \quad \text{strongly in } L^2(0,T;X),$$

and consider problem (72), with $\tilde{\mathbf{v}}$ replaced by $\tilde{\mathbf{v}}_n$. Theorem 1.7 of [1] ensures the existence of a unique weak solution, u_n to such problem. We now obtain some uniform estimates for norms of u_n.

$L^\infty(Q_T)$ estimate. We prove that $\min\{u_{top}, u_0\} \leq u_n \leq 1$ a.e. in Q_T. Using in (72) (with $\tilde{\mathbf{v}}$ replaced by $\tilde{\mathbf{v}}_n$) the admissible test function $T(u_n)$, where T is the Stampaccia truncature function $T(s) = s-1$ for $s > 1$ and $T(s) = 0$ for $s \leq 1$, we obtain, after integration by parts

$$\frac{d}{dt}\int_\Omega \mathcal{T}(u_n) \leq \|\operatorname{div}(\tilde{\mathbf{v}}_n)\|_{L^\infty(Q_T)} \int_\Omega \mathcal{T}(u_n).$$

where $\mathcal{T}$ is the primitive of T with $\mathcal{T}(0) = 0$. Gronwall's Lemma implies $\mathcal{T}(u_n) = 0$ in Q_T, and then $u_n \leq 1$ in Q_T. Since $\tilde{\mathbf{v}}_n \to \tilde{\mathbf{v}}$ strongly in $L^2(0,T;X)$ and $\operatorname{div}\tilde{\mathbf{v}} \in L^\infty(Q_T)$, the estimate $u_n \leq 1$ is valid for all n. To prove $u_n \geq \min\{u_{top}, u_0\}$ one first prove that $u_n \geq 0$ using a Stampaccia truncature function, as above. Then, once we know that $u_n F(\cdot, u_n) \geq 0$, we apply the maximum principle to conclude.

Energy estimate. We use $\varphi = u_n - u_{top} \in L^2(0,T;\mathcal{V}) \cap L^\infty(Q_T)$ as test function. Standard inequalities give us, after integration in $(0,T)$,

$$\frac{1}{4}\int_\Omega {u_n}^2(T) + \frac{1}{2}\int_{Q_T} |\nabla u_n|^2 \leq \frac{1}{2}\int_\Omega u_0^2 + 2\int_{Q_T} {u_n}^2 + 4\int_\Omega u_{top}^2(T) + 4\int_{Q_T} |\tilde{\mathbf{v}}_n|^2 + 4\int_{Q_T} (|u_{top,t}|^2 + |\nabla u_{top}|^2 + u_{top}^2), \quad (73)$$

and Gronwall's Lemma implies

$$\|u_n\|_{L^\infty(L^2)} + \|u_n\|_{L^2(\mathcal{V})} \leq C,$$

with C depending only on norms of u_{top}, u_0 and on the $L^2(Q_T)$ norm of $\tilde{\mathbf{v}}_n$. Observe that since $\tilde{\mathbf{v}}_n \to \tilde{\mathbf{v}}$ strongly in $L^2(Q_T)$, C may be taken independent of n.

Time derivative estimate. Integrating by parts in the convective term of (72) we obtain

$$< u_{nt}, \varphi >= \int_\Omega u_n \operatorname{div}(\varphi \tilde{\mathbf{v}}_n) - \int_\Omega \nabla u_n \cdot \nabla\varphi + \int_\Omega u_n f(\cdot, u_n)\varphi,$$

from where

$$< u_{nt}, \varphi >\leq c_1 \|\nabla\varphi\|_{L^2(\Omega)} + c_2\|\varphi\|_{L^2(\Omega)},$$

with $c_1 = (\|\tilde{\mathbf{v}}_n\|_{L^2(\Omega)} + \|\nabla u_n\|_{L^2(\Omega)})$ and $c_2 = (\|\operatorname{div}\tilde{\mathbf{v}}_n\|_{L^\infty(\Omega)} + \|u_n\|_{L^2(\Omega)})$. Therefore $\|u_{nt}\|_{\mathcal{V}'} \leq C$, with C independent of n for similar reasons than above.

We deduced that the sequence u_n is uniformly bounded with respect to n in the space $L^2(0,T;\mathcal{V}) \cap H^1(0,T;\mathcal{V}') \cap L^\infty(Q_T)$. Therefore, there exists a subsequence u_n and a function $u \in L^2(0,T;\mathcal{V}) \cap H^1(0,T;\mathcal{V}') \cap L^\infty(Q_T)$ such that $u_n \to u$ weakly in $L^2(0,T;\mathcal{V}) \cap H^1(0,T;\mathcal{V}')$ and weakly star in $L^\infty(Q_T)$. In addition, applying Aubin's Lemma we deduce that $u_n \to u$ strongly in $L^2(Q_T)$ and that $u \in C((0,T], L^2(Q_T))$. Passing now to the limit $n \to \infty$ in the formulation (72) is straightforward. □

Theorem 1 *Assume H_1-H_3. Then there exists a weak solution $\mathbf{v} \in L^2(0,T;V) \cap \mathcal{W}_T$, $p \in L^2(0,T;M)$ and $u \in u_{top} + L^2(0,T;\mathcal{V}) \cap H^1(0,T;\mathcal{V}'') \cap L^\infty(Q_T)$ of Problem P, defined as:*

$$a(\mathbf{v},\phi) + b(\phi,p) = -\langle u\mathbf{e}_z,\phi\rangle_\Omega \quad \textit{for all } \phi \in V, \tag{74}$$

$$b(\mathbf{v},q) = -\langle F(\cdot,u),q\rangle_\Omega \quad \textit{for all } q \in M, \tag{75}$$

$$< u_t,\varphi > + R\int_\Omega \varphi\mathbf{v}\cdot\nabla u + \int_\Omega \nabla u\cdot\nabla\varphi = \int_\Omega uF(\cdot,u)\varphi, \quad \textit{for all } \varphi \in \mathcal{V}\cap L^\infty(\Omega) \tag{76}$$

for a.e. $t \in (0,T)$, and with the initial datum satisfied in the sense

$$\lim_{t\to 0} \|u(\cdot,t) - u_0\|_{L^2(\Omega)} = 0.$$

In addition,

$$\min\{u_{top},u_0\} \leq u \leq 1 \quad \textit{a.e. in } Q_T. \tag{77}$$

Proof. We check the hypothesis of the Schauder's fixed point theorem, for the mapping S defined in (53). These are: (i) $S: L^2(Q_T) \to L^2(Q_T)$ is continuous, (ii) S is compact, and (iii) the set

$$\Lambda := \{u \in L^2(Q_T) : u = \lambda S(u), \quad \text{for all } \lambda \in [0,1]\} \quad \text{is bounded.}$$

(i) S is continuous. Consider a sequence $\tilde{u}_n$ such that $\tilde{u}_n \to \tilde{u}$ strongly in $L^2(Q_T)$. We have to prove that $S(\tilde{u}_n) \to S(\tilde{u})$ strongly in $L^2(Q_T)$. We have that $S(\tilde{u}_n) = u_n$ with u_n the solution of problem (72) corresponding to $\tilde{\mathbf{v}}_n$, where $\tilde{\mathbf{v}}_n$ is the first component of the solution of problem (64) corresponding to $\tilde{u}_n$. Lemma 1 implies $\tilde{\mathbf{v}}_n \in L^2(0,T;V) \cap \mathcal{W}_T$ and $\tilde{p}_n \in L^2(0,T;M)$ with uniform bounds in the norms of these spaces. Therefore, Lemma 2 implies that the norms

$$\|u_n\|_{L^\infty(Q_T)}, \quad \|u_n\|_{L^2(0,T;\mathcal{V})}, \quad \|u_{nt}\|_{L^2(0,T;\mathcal{V}'')},$$

are uniformly bounded with respect to n. Hence, there exist functions $u \in u_{top} + L^2(0,T;\mathcal{V}) \cap H^1(0,T;\mathcal{V}'') \cap L^\infty(Q_T)$, $\tilde{\mathbf{v}} \in L^2(0,T;V) \cap \mathcal{W}_T$ and $\tilde{p} \in L^2(0,T;M)$, and subsequences $u_n, \tilde{\mathbf{v}}_n, \tilde{p}_n$ in these spaces such that

$$\tilde{\mathbf{v}}_n \to \tilde{\mathbf{v}} \quad \text{weakly in } L^2(0,T;V), \tag{78}$$

$$\operatorname{div}\tilde{\mathbf{v}}_n \to \operatorname{div}\tilde{\mathbf{v}} \quad \text{weakly star in } L^\infty(Q_T), \tag{79}$$

$$\tilde{p}_n \to \tilde{p} \quad \text{weakly in } L^2(0,T;M), \tag{80}$$

$$u_n \to u \quad \text{weakly star in } L^\infty(Q_T), \tag{81}$$

$$u_n \to u \quad \text{weakly in } L^2(0,T;\mathcal{V}), \tag{82}$$

$$u_{nt} \to u_t \quad \text{weakly in } L^2(0,T;\mathcal{V}''). \tag{83}$$

From (82) and (83) and Aubin's theorem we deduce that

$$u_n \to u \quad \text{strongly in } L^2(Q_T), \quad u \in C([0,T];L^2(\Omega)).$$

From the formulations of problems (64) and (72) we have

$$a(\tilde{\mathbf{v}}_n,\phi) + b(\phi,\tilde{p}_n) = -\langle \tilde{u}_n\mathbf{e}_z,\phi\rangle_\Omega \quad \text{for all } \phi \in V, \tag{84}$$

$$b(\tilde{\mathbf{v}}_n,q) = -\langle F(\cdot,\tilde{u}_n),q\rangle_\Omega \quad \text{for all } q \in M, \tag{85}$$

for a.e. $t \in (0,T)$, and

$$< u_{nt}, \varphi > + \int_\Omega \varphi \tilde{\mathbf{v}}_n \cdot \nabla u_n - \int_\Omega \nabla u_n \cdot \nabla \varphi = \int_\Omega u_n F(\cdot, u_n)\varphi, \tag{86}$$

for all $\varphi \in \mathcal{V} \cap L^\infty(\Omega)$ and for a.e. $t \in (0,T)$. Since, by assumption, $\tilde{u}_n \to \tilde{u}$ strongly in $L^2(Q_T)$ and $f(\mathbf{x},\cdot)$ is continuous for a.e. $\mathbf{x} \in \Omega$, taking the limit $n \to \infty$ in (84)-(85) and using (78)-(80) we obtain

$$a(\tilde{\mathbf{v}}, \phi) + b(\phi, \tilde{p}) = -\langle \tilde{u}\mathbf{e}_z, \phi \rangle_\Omega \quad \text{for all } \phi \in V, \tag{87}$$

$$b(\tilde{\mathbf{v}}, q) = -\langle F(\cdot, \tilde{u}), q \rangle_\Omega \quad \text{for all } q \in M, \tag{88}$$

for a.e. $t \in (0,T)$. Passing to the limit $n \to \infty$ in (86) is straightforward, with the exception of the convective term, since both sequences are only weakly convergent. Integrating by parts, we obtain

$$\int_\Omega \varphi \tilde{\mathbf{v}}_n \cdot \nabla u_n = -\int_\Omega \varphi u_n \operatorname{div} \tilde{\mathbf{v}}_n - \int_\Omega u_n \tilde{\mathbf{v}}_n \cdot \nabla \varphi.$$

For the first term at the right hand side we use that $u_n \to u$ strongly in $L^2(Q_T)$ and that $\operatorname{div} \tilde{\mathbf{v}}_n \to \operatorname{div} \tilde{\mathbf{v}}$ weakly star in $L^\infty(Q_T)$. For the second, again that $u_n \to u$ strongly in $L^2(Q_T)$, that $\|u_n\|_{L^\infty(Q_T)}$ is uniformly bounded, and that $\tilde{\mathbf{v}}_n \to \tilde{\mathbf{v}}$ weakly in $L^2(Q_T)$.

Finally, observe that the uniqueness of solutions of problems (84)-(85) and (86) implies that not only a subsequence but the whole sequence converges.

(ii) S is compact. From the previous analysis, we know that for all $\hat{u} \in L^2(Q_T)$, $u = S(\hat{u}) \in L^2(0,T;\mathcal{V}) \cap H^1(0,T;\mathcal{V}')$, which is compactly embedded in $L^2(Q_T)$, and therefore S is compact.

(iii) Λ is bounded. This property is straightforward to check.

Therefore, the hypothesis of the fixed point theorem are verified and the existence of a weak solution of Problem P is proven. Finally, observe that property (77) is a straightforward consequence of the similar property proven for the sequence u_n of solutions of the concentration problem. □

3 The soil model

A first approximation to the problem is studying the behavior of the system only in the porous medium, assuming that the influence of the water domain may be reduced to its effect on the interface water-porous medium. In this situation, the interface conditions become boundary conditions for the problem in Ω_D. The formulation of the problem is then: Find $u, p : \bar{Q}_T \to \mathbb{R}$ and $\mathbf{v} : \bar{Q}_T \to \mathbb{R}^n$ such that

$$u_t + \operatorname{div}(Ru\mathbf{v} - \nabla u) = 0, \tag{89}$$

$$\operatorname{div} \mathbf{v} + mf(\cdot, u) = 0, \tag{90}$$

$$\mathbf{v} + \nabla p + u\mathbf{e}_z = 0, \tag{91}$$

in $Q_T = \Omega \times (0,T)$, with R and m given by (21). We replace Hypothesis H_1 on the properties of the spatial domain $\Omega_S \cup \Omega_D$ for the following hypothesis for $\Omega = \Omega_D$:

H$'_1$. The spatial domain $\Omega \subset \mathbb{R}^n$ is bounded and its boundary, $\partial\Omega$, is Lipschitz continuous and decomposed as $\partial\Omega = \Gamma_{top} \cup \Gamma_N$, with $\Gamma_{top} \cap \Gamma_N = \emptyset$ and with Γ_{top} of positive $n-1$ dimensional measure.

The rest of hypothesis (H$_2$)-(H$_4$) remain the same with some straightforward modifications. The following boundary conditions are obtained from the transmission conditions of the original problem:

$$u = u_{top}, \quad p = 0 \quad \text{on } \Gamma_{top} \times (0,T), \tag{92}$$

$$\nabla u \cdot \mathbf{n} = \mathbf{v} \cdot \mathbf{n} = 0 \quad \text{on } \Gamma_N \times (0,T). \tag{93}$$

The condition on the pressure is deduced from the balance of normal forces in the water-soil interface, Γ. Indeed, assuming that the velocity in the water is constant, we get from (34) $p_D = p_S$. Moreover, if the concentration in the water, c_S is assumed to be constant too, then from (24) we deduce that p_S does not depend on the horizontal variables and, therefore, p_D equals a constant, say p_{top}, on the interface Γ, which is now the top boundary, Γ_{top} of Ω. Therefore, changing the unknown p to $p - p_{top}$ in (91) and in the boundary condition renders the problem as stated in (89)-(93). Finally, a non-negative initial distribution, u_0, is considered to close the problem

$$u(\cdot,0) = u_0 \quad \text{in } \Omega. \tag{94}$$

The proof of existence of solutions of (89)-(94) is a straightforward modification of Theorem 1 for the water-soil problem, see [23] for details. We start the study of this model by the simplest situation, that of a one-dimensional spatial domain.

3.1 The 1-D model

If the mangroves are uniformly distributed throughout the x,y-plane and there is no lateral fluid flow, a first approach is studying the problem restricted to the one-dimensional z direction in the porous medium domain. By defining $\tilde{v} = Rv$ we see that in the one-dimensional model parameters R and m actually operate as a single parameter

$$m_1 := Rm = \frac{\tau_0 H}{\theta D} \approx (20,200). \tag{95}$$

The problem then reads as follows (omitting tildes). Let $Q_T := \Omega \times (0,T)$ with $\Omega := (0,1)$ and $T > 0$ arbitrarily chosen. Find $u,v : \bar{Q}_T \to \mathbb{R}$ such that

$$u_t + (uv - u_z)_z = 0, \tag{96}$$

$$v_z + m_1 f(\cdot,u) = 0, \tag{97}$$

in Q_T, with the auxiliary data

$$u(0,t) = u_{top}(t), \quad u_z(1,t) = v(1,t) = 0, \quad \text{for } 0 < t < T, \tag{98}$$

$$u(z,0) = u_0(z) \quad \text{for } z \in \Omega. \tag{99}$$

3.2 The 1-D stationary problem

The equilibrium state to which solutions of problem (96)-(99) evolve when $t \to \infty$ is simple enough to give us some quantitative insight in the properties of the model. The problem reads

$$(uv - u')' = 0 \tag{100}$$
$$v' + m_1 f(z,u) = 0, \tag{101}$$

in Ω, with boundary conditions

$$u(0) = u_{top}, \quad u'(1) = v(1) = 0, \tag{102}$$

where primes denote differentiation with respect to z. The existence of solutions of this problem is obtained via a change of unknown together with well known results on the theory of nonlinear equations, see (108) below for the details. For the moment, we concentrate in an interesting qualitative property of the stationary problem which is common to all the models appearing in this work: the existence (*formation*, for evolution problems) of a dead core, i.e., of a non-trivial set in Ω where the salt concentration attains its threshold level $u = 1$. Although we shall prove this property with a high degree of generality in Section 5, we give here a simpler and more intuitive proof for the case of problem (100)-(102).

Integrating equations (100) and (101) in $(z,1)$, using the boundary conditions and assuming that f has the form of example (22) we obtain

$$v(z) = m_1 \int_z^1 f(s,u(s))ds \in (0,m_1], \quad \text{and} \quad u'(z) = u(z)v(z) \geq 0 \quad \text{for } z \in \Omega. \tag{103}$$

In particular, u is an non-decreasing function and therefore, if $u(z_*) = 1$ for some $z_* \in (0,1)$ then $u(z) = 1$ for all $z \in (z_*,1)$. For convenience, we change the unknown u to $\varphi = 1-u$, which satisfies $L_1(\varphi) = 0$, $\varphi(0) = 1-u_{top}$ and $\varphi'(1) = 0$, with

$$L_1(\varphi) = -\varphi'' + v\varphi' + m_1 k(z)(1-\varphi)\varphi^r.$$

To show conditions under which $\varphi = 0$ (i.e. $u = 1$) in some subset of Ω we use the comparison principle which states that if ψ is a solution of

$$-L_1(\psi) \geq 0, \quad \psi(0) = 1-u_{top} \quad \text{and} \quad \psi'(1) = 0, \tag{104}$$

then $\psi \geq \varphi$ in Ω. Therefore, if we are able to construct a solution of (104) such that $\psi(z) = 0$ for $z \in (z_*,1)$ then it necessarily holds $\varphi(z) = 0$ for $z \in (z_*,1)$. In the following theorem we give conditions under which a supersolution of (104) vanishing in Ω does exist.

Theorem 2 *Let (u,v) be a solution of (100)-(102) corresponding to f given by (22) and define*

$$\xi(r) = 2\frac{1+r}{(1-r)^2} + \frac{2m_1}{1-r}.$$

Assume that the data problem satisfy

$$\frac{(1-u_{top})^{1-r}}{u_{top}} < \frac{m_1}{\xi(r)}. \tag{105}$$

Then there exists $z_* < 1$ such that $u(z) = 1$ for $z \in (z_*,1)$.

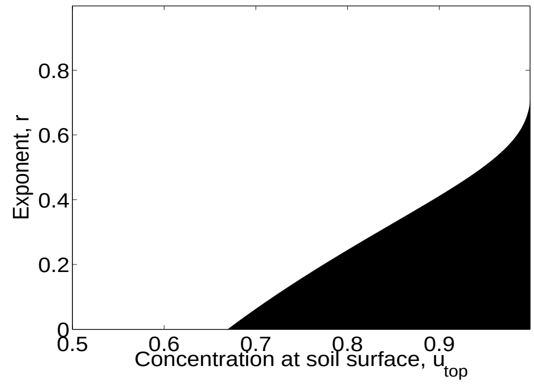

Figure 2. In black, region of validity of inequality (105) for $m_1 = 100$.

Proof. We have that (103) implies $v\psi' \geq m_1\psi'$ and therefore, if ψ satisfies $L_2(\psi) \geq 0$, $\psi(0) = 1 - u_{top}$ and $\psi'(1) = 0$, with

$$L_2(\psi) = -\psi'' + m_1\psi' + m_1(1-\psi)k(z)\psi^r, \tag{106}$$

then it also satisfies (104). Consider the function

$$\psi(z) := \begin{cases} a(z_* - z)^{\frac{2}{1-r}} & \text{if } z \in (0, z_*), \\ 0 & \text{if } z \in (z_*, 1). \end{cases} \tag{107}$$

Then, the boundary conditions imply $z_* = \left(\frac{1-u_{top}}{a}\right)^{(1-r)/2}$, and a necessary condition for a dead core of positive measure to exist is $z_* < 1$, i.e., $a > 1 - u_{top}$. For $z < z_*$, we have

$$L_2(\psi(z)) = (z_* - z)^{2r/(1-r)} a^r \Big(m_1 - a^{1-r}\big(2\frac{1+r}{(1-r)^2} + \frac{2m_1}{1-r}(z_* - z)\big) - m_1 a (z_* - z)^{2/(1-r)} \Big).$$

Since $r < 1$ and $z_* - z$ and a must be positive, we have that if

$$m_1 \geq a^{1-r}\xi(r) + m_1 a,$$

then $L_2(\psi(z)) \geq 0$. Therefore, we search for conditions for a satisfying

$$1 - u_{top} < a < 1 \quad \text{and} \quad \frac{a^{1-r}}{1-a} \leq \frac{m_1}{\xi(r)}.$$

Since the function $a^{1-r}/(1-a)$ is increasing, it suffices to have (105) □

Regarding the existence of solutions, observe that from (103) and the boundary data $u(0) = u_{top}$ we obtain that $u \geq u_{top}$ in Ω. As mentioned in Remark 1, the case $u_{top} = 0$ leads to the trivial solution $u = 0$. Therefore, we assume $u_{top} > 0$, which allow us to define

$$w(z) := \log u(z) \quad \text{for } z \in \bar{\Omega}, \tag{108}$$

for which we find the boundary value problem

$$w'' + g(z, w) = 0 \quad \text{for } z \in \Omega, \quad w(0) = \log u_{top}, \quad w'(1) = 0, \tag{109}$$

Table 2. Data for numerical experiments

Experiment	1	2	3	4	5	6	7	8
u_{top}	0.25	0.25	0.25	0.25	0.50	0.50	0.50	0.50
m_1	20	20	200	200	20	20	200	200
r	1	0.5	1	0.5	1	0.5	1	0.5

with $g(z,w) := m_1 f(z,e^w)$. As a consequence of Hypothesis H_2, function g satisfies:

$$\begin{cases} \text{(a) } g(z,\cdot) \in C((-\infty,0]) \text{ for a.e. } z \in \Omega; \\ \text{(b) } g(\cdot,s) \in L^\infty(\Omega) \text{ for all } s \in (-\infty,0]; \\ \text{(c) } g(z,\cdot) \text{ is non-increasing in } (-\infty,0] \text{ and } g(z,0) = 0 \text{ for a.e. } z \in \Omega. \end{cases}$$

We can apply well-known results (see, e.g., [18]) to prove the existence of solutions of problem (109) in the class $W^{1,1}(\Omega)$. By the additional regularity in (b) it is straightforward to show that solutions of (109) belong to $W^{2,\infty}(\Omega)$ (note that $W^{1,1}(\Omega) \subset L^\infty(\Omega)$ in one space dimension). Finally, due to (c), we observe that the solution of (109) depends monotonically in u_{top}. We also point out that the possible non-Lipschitz continuity of $f(z,\cdot)$ carries over to $g(z,\cdot)$.

A numerical experiment. We used formulation (109) to construct a discrete scheme, based on Newton's method, for approximating solutions of the steady problem (96)-(99). Data was fixed as follows. We used two extremal values for the extraction number $m_1 = \tau_0 H/\theta D$, $m_1 = 20$ and $m_1 = 200$. Since we take the depth of the domain as $H = 1\,\mathrm{m}$ (roots occupying the first 25 cm, i.e. $d = 0.25$), the porosity $\theta = 0.5$, and the diffusion coefficient as $D = 10^{-9}\,\mathrm{m}^2\,\mathrm{s}^{-1}$, the above values of m_1 imply $\tau_0 = 10^{-7}\,\mathrm{m\,s}^{-1}$ and $\tau_0 = 10^{-8}\,\mathrm{m\,s}^{-1}$, respectively, which is in good concordance with experimental data, see [46]. We also play with the value of salt concentration at the top boundary: $u_{top} = 0.25$, corresponding to a 50-50 mixture of fresh water and sea water, and $u_{top} = 0.5$, corresponding to sea water salt concentration. Finally, values $r = 0.5$ and $r = 1$ of the power in function f are explored. More concretely, we test our model in eight experiments corresponding to data on Table 2 We show the results in Figure 3. We observe that the variation of parameters m_1 and r has qualitatively different results. While power r on function f determines the possibility of concentration reaching the threshold value $u = 1$ according to values $r \geq 1$ or $r < 1$, its effect on the quantitative increment of salt concentration is not as large as the variation on m_1, the parameter expressing the strength of the fresh water uptaking.

3.3 The 1-D evolution problem

Existence of solutions of the one-dimensional evolution problem (96)-(99) is again a straightformward consequence of Theorem 1. However, due to the great simplification which involves considering the mass conservation equation $\operatorname{div} \mathbf{v} = mf(\cdot,u)$ in one space dimension, which allows to eliminate the Darcy's law from the problem, the solutions of (96)-(99) may be shown to be *strong* solutions, i.e., functions (u,v) which satisfy (96)-(99) in the sense of $L^2(Q_T)$ and not just in a weak sense. In fact, if the boundary and initial data

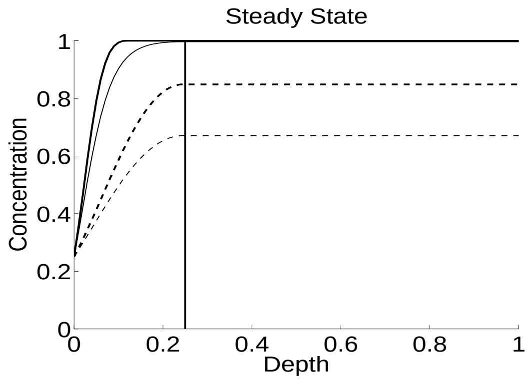

(a) Experiments (1) to (4)

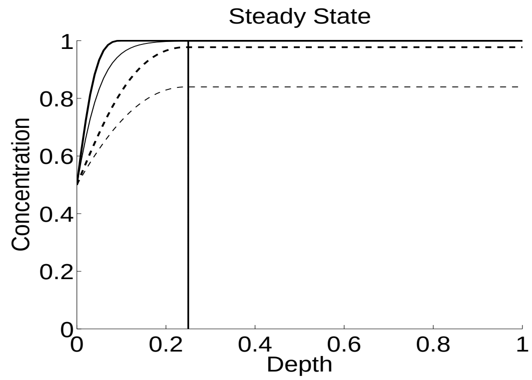

(b) Experiments (5) to (8)

Figure 3. Salt concentration corresponding to Experiments 1-8. Curves are ordered increasingly according to experiment number. Solid and dotted curves correspond to $m_1 = 200$ and $m_1 = 20$, respectively. Among them, concentration corresponding to $r = 0.5$ is always above that corresponding to $r = 1$. Vertical line is roots depth.

are smooth enough and satisfy certain compatibility condition and if we assume, as usual, a functional form for f of the type (22) then we have, as a result of classical regularity theory, see [39],

$$u \in C^{2+r,1+\frac{r}{2}}(\bar{Q}_T),$$
$$v \in C^{1+r,r}(\bar{Q}_T).$$

3.3.1 Qualitative properties of solutions

Theorem 3 *1.* Uniqueness of solutions. *Let (u_1, v_1) and (u_2, v_2) be two strong solutions of problem (96)-(99). If either*

$$f(z,\cdot) \quad \text{is Lipschitz continuous in } [0,1] \quad \text{for almost all } z \in \Omega, \tag{110}$$

or anyone of the solutions satisfies

$$u(z,t) > \int_0^z |u_z(y,t)|\, dy \quad \text{a.e. in } Q_T, \tag{111}$$

then $(u_1, v_1) = (u_2, v_2)$ a.e. in Q_T.

2. Comparison of solutions. *Assume now that (u_1, v_1) and (u_2, v_2) correspond to ordered data, i.e. $u_{1,top} \le u_{2,top}$ in $(0,T)$ and $u_{10} \le u_{20}$. Then, if*

$$u_{iz} \ge 0 \quad \text{in } Q_T \qquad \text{and} \qquad u_{i,top} > 0 \quad \text{in } (0,T], \tag{112}$$

for either $i = 1$ or $i = 2$, then

$$u_1 \le u_2 \quad \text{and} \quad v_1 \ge v_2 \quad \text{in } Q_T.$$

Remark 2 1. By (103) we have that the solution of the stationary problem is monotonic in space. Theorem 3 implies then that if $(u_{1,top}, u_{10}) \le (U_{top}, U) \le (u_{2,top}, u_{20})$, where (U,V) is the stationary solution corresponding to the boundary data U_{top}, then

$$u_1 \le U \le u_2 \quad \text{and} \quad v_1 \ge V \ge v_2 \quad \text{in } Q_T.$$

2. For both (110) and (111) it is unclear why they should influence the uniqueness of solutions. We believe that both are in fact only technical restrictions, and that uniqueness should hold under weaker assumptions on f and u.

Remark 3 Since inequality (111) is difficult to verify directly, the following observation is useful, see [22] for the proof. Let f be given by (22) and assume $u_0 \equiv u_{top} = \tilde{u}$, with

$$\tilde{u} > \max\left\{\frac{2}{2+r}, 1-(m_1)^{-r}\right\} \tag{113}$$

Then *(111)* holds.

The following theorem, proved in [22], answers the question of convergence of the time dependent solution to the steady state solution. For simplicity we confined ourselves to the case of constant boundary data, i.e.

$$u_{top} \equiv \tilde{u} \in (0,1) \tag{114}$$

and let (U,Q) be the stationary solution corresponding to this boundary condition. Since U is increasing in z, it is admissible as a comparison function by, Theorem 3. Therefore, if the initial data, u_0, and U are ordered, e.g. $u_0 \le U$, then this ordering persists through time: $u(z,t) \le U(z)$ for all $z \in \Omega$ and $t > 0$. This property allows us to prove the

Theorem 4 *Let (u,v) be a solution of problem (96)-(99) and let (U,V) be the corresponding steady state solution of problem (100)-(102). Let u_0 and U be ordered, i.e. either $u_0(z) \le U(z)$ for all $z \in \Omega$, or $u_0(z) \ge U(z)$ for all $z \in \Omega$. Then*

$$\begin{array}{l} u(\cdot,t) \to U \\ v(\cdot,t) \to V \end{array} \qquad \text{as } t \to \infty,$$

uniformly in Ω.

Proof of Theorem 3. Since the constant m_1 do not play any role in this proof we set $m_1 = 1$, for clarity. We first discuss the proof of part 1. Let (u_1, v_1) and (u_2, v_2) be solutions of problem (96)-(99) and set $(u,v) = (u_1 - u_2, v_1 - v_2)$. Then (u,v) satisfies

$$\left\{\begin{array}{ll} \left.\begin{array}{l} u_t + (uv_1 + u_2 v)_z - u_{zz} = 0 \\ v_z + f(z,u_1) - f(z,u_2) = 0 \end{array}\right\} & \text{a.e. in } Q_T, \\ \text{with} & \\ \left.\begin{array}{l} u_{top}(0,\cdot) = 0 \\ u_z(1,\cdot) = v(1,\cdot) = 0 \end{array}\right\} & \text{in } (0,T), \\ u_0 = 0 \quad \text{in} \quad \Omega. & \end{array}\right. \tag{115}$$

Multiplying the differential equations of (115) by smooth functions φ,ψ satisfying

$$\varphi(0,t)=\varphi_z(1,t)=\psi(0,t)=0 \quad \text{for any } t\in[0,T], \tag{116}$$

integrating in Q_τ, with $\tau\in(0,T)$, and adding the resulting integral identities we obtain

$$\begin{aligned}\int_\Omega u(\tau)\varphi(\tau) &= \int_{Q_\tau} u\left(\varphi_t+v_1\varphi_z+\varphi_{zz}\right)-\int_{Q_\tau} v\left(\psi_z+u_{2z}\varphi\right)\\ &+\int_{Q_\tau}\left(f(z,u_1)-f(z,u_2)\right)\left(u_2\varphi+\psi\right).\end{aligned} \tag{117}$$

We consider the function

$$h(z,t):=\begin{cases}\dfrac{f(z,u_1(z,t))-f(z,u_2(z,t))}{u(z,t)} & \text{if} \quad u(z,t)\neq 0,\\ 0 & \text{if} \quad u(z,t)=0,\end{cases} \tag{118}$$

which is non-positive because $f(z,\cdot)$ is non-increasing. For $m\in\mathbb{N}$, $m\geq 1$, we consider the functions $hH(h+m)$, where H denotes the Heaviside function: $H(s)=1$ for $s\geq 0$, $H(s)=0$ for $s\leq 0$. We regularize these functions in such a way that we obtain a smooth sequence $\{h^m\}\subset C^2(Q_\tau)$ satisfying

(i) $h^{m+1}\leq h^m$ in Q_τ,

(ii) $0\geq h^m\geq \max\{-m,h\}$,

(iii) $h^m\to h$ a.e. in Q_τ.

The regularity of solutions of problem (96)-(99) allows us to introduce sequences $\{v_1^n\}_{n\geq 1}$, $\{u_2^n\}_{n\geq 1}\subset C^2(Q_T)$ such that

$$v_1^n\to v_1 \quad \text{and} \quad u_2^n\to u_2 \quad \text{strongly in } L^2(0,T;H^1(\Omega)) \tag{119}$$

as $n\to\infty$ with

$$\begin{aligned}&\overline{\lim}\,\|v_1^n\|_{L^\infty(Q_T)}\leq\|v_1\|_{L^\infty(Q_T)}, \quad \overline{\lim}\,\left\|v_{1z}^n\right\|_{L^2(Q_T)}\leq\|v_{1z}\|_{L^2(Q_T)},\\ &\overline{\lim}\,\|u_2^n\|_{L^\infty(Q_T)}\leq\|u_2\|_{L^\infty(Q_T)}, \quad \overline{\lim}\,\left\|u_{2z}^n\right\|_{L^2(Q_T)}\leq\|u_{2z}\|_{L^2(Q_T)},\end{aligned} \tag{120}$$

and u_2^n satisfying (111). Using these approximations we rewrite (117) as

$$\begin{aligned}\int_\Omega u(\tau)\varphi(\tau) = &\int_{Q_\tau} u\left(\varphi_t+v_1^n\varphi_z+\varphi_{zz}+h^m\left(u_2^n\varphi+\psi\right)\right)-\int_{Q_\tau} v\left(\psi_z+u_{2z}^n\varphi\right)\\ &+\int_{Q_\tau} u\left(h-h^m\right)\left(u_2\varphi+\psi\right)-\int_{Q_\tau} u_z\left(v_1-v_1^n\right)\varphi\\ &-\int_{Q_\tau} u(v_{1z}-v_{1z}^n)\varphi+\int_{Q_\tau} uh^m\left(u_2-u_2^n\right)\varphi-\int_{Q_\tau} v\left(u_{2z}-u_{2z}^n\right)\varphi.\end{aligned} \tag{121}$$

Next we select the functions φ and ψ, being solutions of

$$\begin{cases}\left.\begin{array}{l}\varphi_t+v_1^n\varphi_z+\varphi_{zz}+h^m\left(u_2^n\varphi+\psi\right)=0\\ \psi_z+u_{2z}^n\varphi=0\end{array}\right\} \quad \text{in } Q_\tau,\\ \varphi(\tau)=\xi \quad \text{in } \Omega,\end{cases} \tag{122}$$

with φ,ψ satisfying (116) and with $\xi\in C_0^\infty(\Omega)$, $\xi\geq 0$.

Lemma 3 *(i) Assume either* (110) *or* (111). *Then, for each n and m there exists a unique solution* $\varphi,\psi \in C^{2,1}(\bar{Q}_\tau)$ *of* (122) *such that* $\|\varphi\|_{L^\infty(Q_\tau)}$ *and* $\|\psi\|_{L^\infty(Q_\tau)}$ *are uniformly bounded with respect to n and m.*

(ii) Assume (112). *Then, in addition to the uniform bounds we have*

$$\varphi \geq 0 \quad in\ Q_T \quad and \quad \varphi_z(0,t) \geq 0 \quad in\ (0,T). \tag{123}$$

End of proof of Theorem 3. Using the functions provided by Lemma 3 we obtain from (121)

$$\int_\Omega u(\tau)\xi = \int_{Q_\tau} u\,(h-h^m)\,(u_2\varphi+\psi) - \int_{Q_\tau} u_z\,(v_1-v_1^n)\,\varphi \\ - \int_{Q_\tau} u(v_{1z}-v_{1z}^n)\varphi + \int_{Q_\tau} uh^m\,(u_2-u_2^n)\,\varphi - \int_{Q_\tau} v\,\left(u_{2z}-u_{2z}^n\right)\varphi. \tag{124}$$

By the uniform estimates from Lemma 3 and (120), we can pass to the limit in (124) and obtain for $n \to \infty$

$$\int_\Omega u(\tau)\xi = \int_{Q_\tau} u\,(h-h^m)\,(u_2\varphi+\psi)\,. \tag{125}$$

Using Lemma 3 again and the convergence properties of the sequence $\{h^m\}$ we find

$$\int_{Q_\tau} u\,(h-h^m)\,(u_2\varphi+\psi) \to 0 \quad \text{as} \quad m \to \infty, \tag{126}$$

and hence we obtain from (125)

$$\int_\Omega u(\tau)\xi = 0, \tag{127}$$

for any test function $\xi \geq 0$. We therefore deduce that $u_1 = u_2$ a.e. in Q_τ for any $\tau \in (0,T)$. Checking that this implies $v_1 = v_2$ is straightforward.

To prove part 2 we define again $(u,v) := (u_1-u_2, v_1-v_2)$ and consider the problem for (u,v) given by (115) but with $u_{top} := u_{1,top} - u_{2,top} \leq 0$ and $u_0 := u_{10} - u_{20} \leq 0$. Following the proof of part 1 we get

$$\int_\Omega u(\tau)\varphi(\tau) \quad = \int_\Omega u_0\varphi(0) + \int_0^T u_{top}(t)\varphi_z(0,t)dt + I_1, \tag{128}$$

with I_1 given by the right hand side of (121). By Lemma 3 the solution (φ,ψ) of (122) satisfies $\varphi(0,t) \geq 0$ and $\varphi_z(0,t) \geq 0$. Hence, we obtain from (128) and (122)

$$\int_\Omega u(\tau)\xi \leq 0,$$

for all $\xi \geq 0$, from where the assertion follows. □

Proof of Lemma 3. Because (122) is linear with smooth coefficients and data, existence, uniqueness and regularity of solutions is well known [39]. To show the uniform L^∞ bounds we consider separately the cases (110) and (111). If (110) holds, then h defined by (118) is bounded, and consequently, $\{h^m\}$ is uniformly bounded in $L^\infty(Q_\tau)$ with respect to m.

Further, (120) ensures that v_1^n, u_2^n and u_{2z}^n are uniformly bounded in $L^\infty(Q_\tau)$ with respect to n.

Next assume (111). We assert that the global maximum of $|\varphi|$ is attained either at the boundary $z=0$ or initially at $t=\tau$ implying $\|\varphi\|_{L^\infty(Q_\tau)}$ uniformly bounded with respect to m and n. Suppose this is not true. Let $(z_0,\tau_0)\in Q_\tau$ be the point where the global maximum of $|\varphi|$ is attained. Then (z_0,τ_0) is either a point of global maximum or a point of global minimum for φ. Let us consider first the case in which (z_0,τ_0) is a point of global maximum. The boundary data for φ implies $\varphi(z_0,\tau_0)>0$ and the φ–equation in (122) yields, using $h^m\le 0$,

$$u_2^n(z_0,\tau_0)\varphi(z_0,\tau_0)+\psi(z_0,\tau_0)\le 0. \tag{129}$$

Integrating the ψ–equation of (122) in $(0,z)$ gives

$$\psi(z,t)=\int_0^z\left(-u_{2z}^n(y,t)\right)\varphi(y,t)dy. \tag{130}$$

Therefore, from (129), (130) and assumption (111) we obtain

$$\begin{aligned}u_2^n(z_0,\tau_0)\varphi(z_0,\tau_0)&\le\int_0^{z_0}u_{2z}^n(y,\tau_0)\varphi(y,\tau_0)dy\\&\le\int_0^{z_0}\left|u_{2z}^n(y,\tau_0)\right|dy\sup_{y\in(0,z_0)}|\varphi(y,\tau_0)|\\&=\int_0^{z_0}\left|u_{2z}^n(y,\tau_0)\right|dy\,\varphi(z_0,\tau_0)<u_2^n(z_0,\tau_0)\varphi(z_0,\tau_0),\end{aligned} \tag{131}$$

a contradiction. If the global maximum is attained at a point $(1,\tau_0)$, then by the strong maximum principle $\varphi_z(1,\tau_0)>0$. This gives again a contradiction. Finally, if (z_0,τ_0) is a point of global minimum for φ, we may repeat the argument above obtaining a similar contradiction. To finish the proof of (i) we use (130) and (120) to find

$$\|\psi\|_{L^\infty(Q_\tau)}\le\|\varphi\|_{L^\infty(Q_\tau)}\|u_2\|_{L^\infty(0,\tau;W^{1,1}(\Omega))},$$

which is also independent of m and n.

The proof of (ii) follows the same ideas as that of (i). We assume (112) and assert that the global minimum of φ is attained either at the boundary $z=0$ or initially at $t=\tau$ implying (123), see (116) and (122). Suppose this is not true. Then, using the arguments of part (i) for the function φ instead of $|\varphi|$, we are led to an expression similar to (131):

$$\begin{aligned}u_2^n(z_0,\tau_0)\varphi(z_0,\tau_0)&\ge\int_0^{z_0}u_{2z}^n(y,\tau_0)\varphi(y,\tau_0)dy\\&\ge\int_0^{z_0}u_{2z}^n(y,\tau_0)dy\inf_{y\in(0,z_0)}\varphi(y,\tau_0))>u_2^n(z_0,\tau_0)\varphi(z_0,\tau_0),\end{aligned}$$

a contradition. □

3.3.2 Numerical simulations

For the numerical solution of problem (96)-(99) we considered the equivalent non-local formulation

$$\begin{cases} u_t + m_1 \left(u \int_z^1 f(\cdot,u) \right)_z - u_{zz} = 0 & \text{in } Q_T, \\ u(0,t) = u_{top}(t), \quad u_z(1,t) = 0 & \text{for } 0 < t < T, \\ u(z,0) = u_0(z) & \text{for } 0 < z < 1, \end{cases} \tag{132}$$

which is obtained after the integration in $(z,1)$ of equation (97). To compute approximate solutions we employed the following semi-implicit finite difference scheme

$$u^{\tau+1} - \tau u_{zz}^{\tau+1} = u^\tau + \tau m_1 \big(u^\tau f(\cdot,u^\tau) - u_z^\tau \int_z^1 f(\cdot,u^\tau) \big),$$

with $\tau = 0,1,\cdots$ and $u^0 = u_0$. Parameters were fixed as in the simulations of the solutions of the steady state problem, see page 26. We run six numerical experiments corresponding to the data shown in Table 3.

Table 3. Data for numerical experiments

Experiment	1	2	3	4	5	6
$u_0 = u_{top}$	0.25	0.25	0.5	0.5	0.50	0.25
m_1	20	20	200	200	20	200
r	1	0.5	1	0.5	0.5	1

In Figure 4 we show the results of Experiments 1-6 for salt concentration at times $t \approx 0,\ 5,\ 10,\ 20,\ 40$ years. In Plot (b) of that figure, we see that condition $r < 1$ for the formation of a dead core is not sufficient and that, in fact, it seems to be more relevant for the rapid increase of the salt concentration a high combination of Rayleigh and extraction numbers (the number m_1) than the power value. Physically, this corresponds to the situation in which the porous medium is relatively highly permeable and the mangroves' transpiration rate is high enough.

In particular, in Experiment 5, we take high initial data $u_0 = 0.5$, very low Rayleigh-extraction number $m_1 = 20$ and $r = 0.5$, which could give rise to a dead core. Experiment 6 runs with a smaller initial data, $u_0 = 0.25$, a linear exponent in the extraction function but a large m_1 $(= 200)$. We observe that in both cases the behavior of the concentration after ten years is very similar, with a profile of high salinization.

In Plots (a)-(b) and (c)-(d), which share the same value of m_1 and initial data, solutions corresponding to lower r are greater, i.e, salt concentration depends in a decreasing way on the power of the extraction function. This is specially noticeable in Plots (a)-(b), where the steady state is below the salt concentration threshold.

In Figure 5 we plot the water discharges corresponding to Experiments 5 and 6 for $t = 5$ years (dotted line) and $t = 40$ year (continuous line). We check that the water inflow in the porous medium is much higher in the case of small boundary salt concentration data due to the greater ability of mangroves' roots to uptake fresh water.

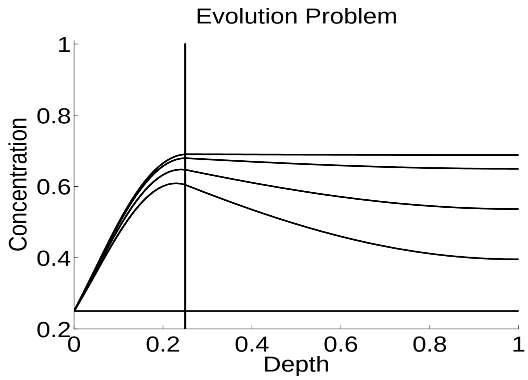

(a) Experiment 1. $u_0 = 0.25$, $m_1 = 20$ and $r = 1$.

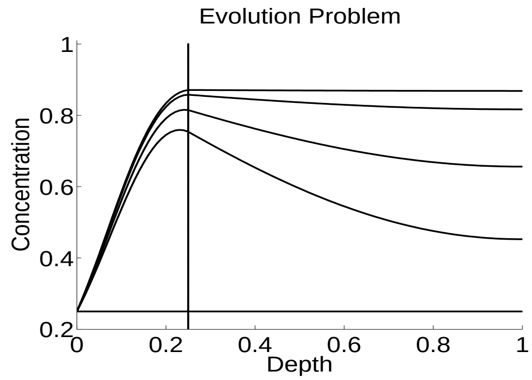

(b) Experiment 2. $u_0 = 0.25$, $m_1 = 20$ and $r = 0.5$.

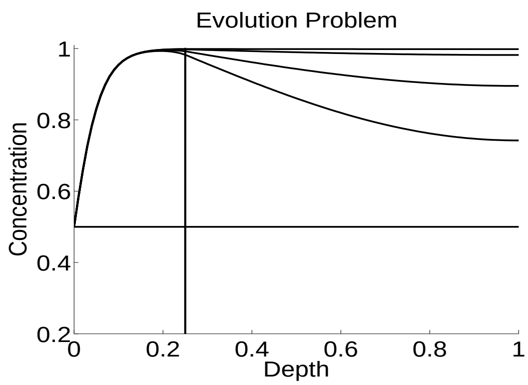

(c) Experiment 3. $u_0 = 0.5$, $m_1 = 200$ and $r = 1$.

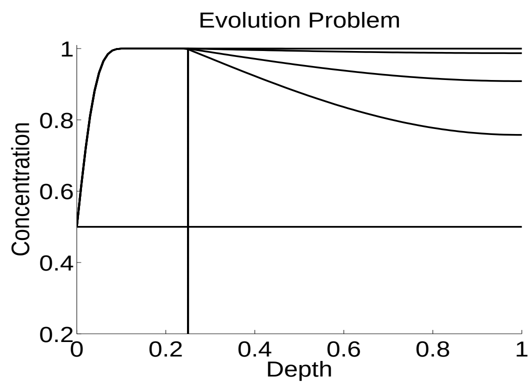

(d) Experiment 4. $u_0 = 0.5$, $m_1 = 200$ and $r = 0.5$.

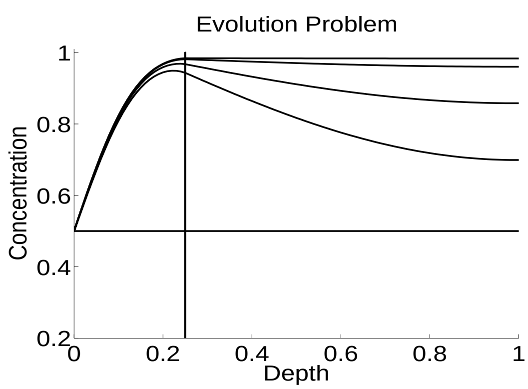

(e) Experiment 5. $u_0 = 0.5$, $m_1 = 20$ and $r = 0.5$.

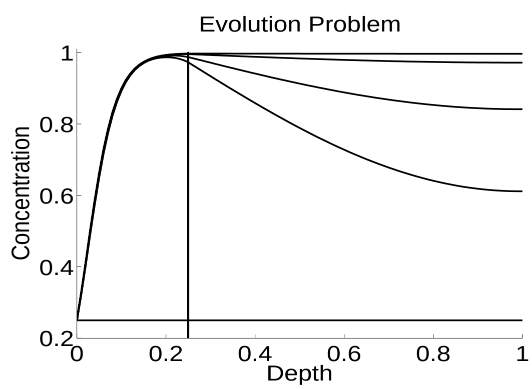

(f) Experiment 6. $u_0 = 0.25$, $m_1 = 200$ and $r = 1$.

Figure 4. Evolution of salt concentration corresponding to Experiments 1-6. Curves correspond to increasingly ordered salt concentration at times, $t \approx 0,\ 5,\ 10,\ 20,\ 40$ years. Vertical line is the roots depth.

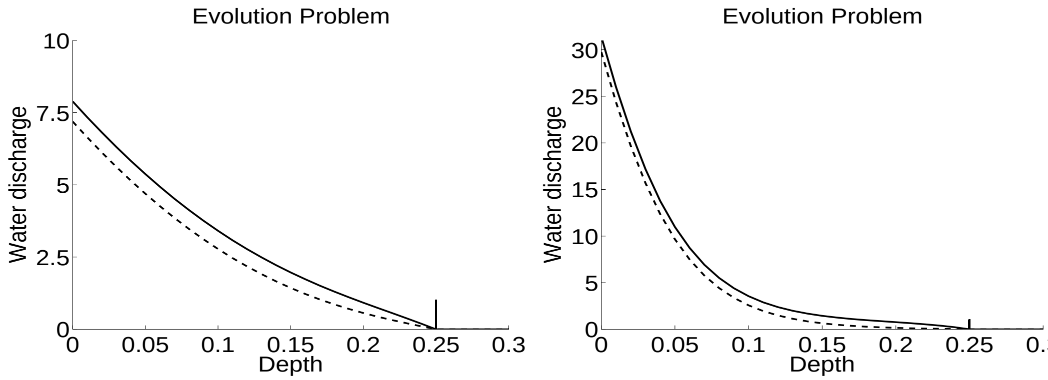

(a) Experiment 5. $u_0 = 0.5$, $m_1 = 20$ and $r = 0.5$. (b) Experiment 6. $u_0 = 0.25$, $m_1 = 200$ and $r = 1$.

Figure 5. Water discharge in the root zone. Continues line corresponds to $t = 5$ years and dotted line to $t = 40$ years.

3.4 Stability analysis

A similar result than Theorem 2, on the formation of a fully salinized region for the steady state solution, will be proven in Section 5, see Theorem 7, for the evolution problem: if the exponent r in function f, see (22), is smaller than one then the solute concentration may reach the threshold value $u = 1$ in some subset of $(0,1)$ in finite time, while $u < 1$ below that layer. In fact, this has already been numerically demonstrated in Section 3.3.2. This is clearly an instable situation and it is therefore expectable to observe gravitational instabilities when perturbations of the one-dimensional profile are considered in the n-dimensional setting. Our aim is to provide a range of values for the bifurcation parameter, R, for which these instabilities appear.

The stability properties of equations (89)-(91) has received attention for a variety of data, and phenomena like cellular convection or fingering have been proven to arise when the bifurcation parameter, R, is large enough. For instance, the steady state one-dimensional solution of the model problem with $L = \infty$, $f = 0$, $\mathbf{v} \cdot \mathbf{n} = 0$ on $\partial\Omega \times (0,T)$ and $u = 1$ on $\Gamma_{top} \times (0,T)$ is known to be instable for values $R > 4\pi^2$, see for instance [56]. Other interesting models related to ours which also lead to gravitational instabilities are the salt lake formation by evaporation ($\mathbf{v} \cdot \mathbf{n} = -const.$ on $\Gamma_{top} \times (0,T)$), see [24], or the peat moss formation ($f = 0$ and the temperature $u = u_{top}(t)$ on Γ_{top}), see [60]. The common feature of these models is the existence of an instable ground state, i.e., a steady one-dimensional solution which may be gravitationally instable. Analysis of the perturbation equations (linearized or not) and the study of a maximization problem for the bifurcation parameter is the usual approach for finding the threshold value of R above which instabilities occur.

For problem (89)-(94), due to the non-zero extraction term f and to the non-flow boundary condition $\mathbf{v} \cdot \mathbf{n} = 0$ on $\Gamma_N \times (0,T)$, the one-dimensional steady state solution is stable, see Section 3.2. The mathematical explanation for such a stable solution after a possibly instable transient state is given by the non-flow boundary condition at the bottom of the domain, condition which allows the salt *produced* in the extraction zone to fill up the region below this zone till the bottom boundary in infinite time.

A rigorous mathematical analysis of the existence of transient instabilities is out of our scope but its physical interest, which resides in the shortening of the time rate at which solutions to the evolution problem approach to the steady state, motivate us to study certain approximations which may be treated rigorously, and to demonstrate by means of numeric simulations that the behavior of solutions to the approximated problems and to the original problem are similar, at least in the selected parameters range.

Therefore, to give some clues to this question, we shall consider a related problem which is simpler to deal with but which keeps relevant information about solutions of problem (89)-(94). In this section and for the numerics, we fix $n = 2$, although it is not an essential assumption for the analysis that follows.

We consider the situation in which, after some time $T^* < T$, the solution to the one-dimensional problem has developed a dead core, i.e., an interval $(a,b) \subset (0,1)$ in which $u = 1$ for all $t > T^*$. For simplicity, we assume $b = d$, being $(0,d)$ the root zone, which is a reasonable assumption, see Figure 4. Following, we investigate the stability of this one-dimensional configuration in the two-dimensional setting, with a modified boundary condition on the bottom, $z = 1$. Consider the domain free of roots $\Omega_d = (0,L) \times (d,1)$, where $f \equiv 0$. The top boundary, $z = d$, corresponds to the boundary between the dead core and the no-extraction region so we prescribe $u = 1$ on this boundary. On the bottom boundary, $z = 1$, we take constant Dirichlet data $u^* < 1$ instead of the non-flow boundary data, assuming that the value of u in $z = 1$ for the one-dimensional problem does not vary too fast for the time scale of the transient instabilities we are studying. Therefore, we set the following boundary conditions

$$u(x,d,t) = 1, \quad u(x,1,t) = u^* \quad \text{for } x \in (0,L) \tag{133}$$

$$p(x,d,t) = p_0, \quad v_2(x,1,t) = 0 \quad \text{for } x \in (0,L), \tag{134}$$

$$\frac{\partial u}{\partial x}(0,z,t) = \frac{\partial u}{\partial x}(L,z,t) = 0 \quad \text{for } z \in (d,1), \tag{135}$$

$$v_1(0,z,t) = v_1(L,z,t) = 0 \quad \text{for } z \in (d,1), \tag{136}$$

for $t > T^*$, $\mathbf{v} = (v_1, v_2)$ and a constant p_0. Since T^* will not play any important role in the analysis, we set $T^* = 0$. In the domain $\Omega_d \times (0,T)$, functions $(u, \mathbf{v}, p)$ satisfy

$$u_t + R\mathbf{v} \cdot \nabla u - \Delta u = 0, \tag{137}$$

$$\operatorname{div} \mathbf{v} = 0, \tag{138}$$

$$\mathbf{v} + \nabla p + u\mathbf{e}_z = 0. \tag{139}$$

Stability conditions for equations (137)-(139) is a well known issue and has been established for different types of boundary conditions, see the monographes of Straughan [56,57] and the references therein . In fact, problem (133)-(139) only differs from the one treated in [56] in two points: the domain is bounded in the horizontal direction ($L < \infty$) and the non-flow boundary condition on the top domain, $v_2(x,d,t) = 0$ of [56] is replaced by our condition on the pressure $p(x,d,t) = p_0$. The stability analysis is based on the expansion

$$\tilde{u} = U_0 + u, \quad \tilde{\mathbf{v}} = V_0 + \mathbf{v} \quad \text{and} \quad \tilde{p} = P_0 + p, \tag{140}$$

with $\tilde{u}$, $\tilde{\mathbf{v}}$ and $\tilde{p}$ satisfying problem (133)-(139) and with U_0, V_0 and P_0 the solution to the corresponding one dimensional steady state problem, given by

$$U_0(z) = 1 - \gamma(z - d), \quad V_0(z) = 0, \quad P_0(z) = p_0 + \int_d^z U_0(s)ds,$$

for $z \in (d,1)$ and $\gamma = (1-u^*)/(1-d)$. Substituting (140) into equations (137)-(139) and omitting tildes, yields the following system for the perturbations

$$u_t + R\mathbf{v}\cdot\nabla u - \Delta u = \gamma R v_2, \tag{141}$$

$$\operatorname{div}\mathbf{v} = 0, \tag{142}$$

$$\mathbf{v} + \nabla p + u\mathbf{e}_z = 0, \tag{143}$$

in $\Omega_d \times (0,T)$, satisfying the homogeneous boundary conditions corresponding to (133)-(136). Conditions for nonlinear stability are deduced in the usual way. Multiplying (141) by u, integrating by parts and using (142) and the boundary conditions we obtain

$$\frac{1}{2}\frac{d}{dt}\int_{\Omega_d} u^2 + \int_{\Omega_d} \nabla u^2 = \gamma R \int_{\Omega_d} v_2 u. \tag{144}$$

Multiplying (143) by $\alpha\mathbf{v}$, $\alpha > 0$ and adding the result to (144) we obtain

$$\frac{1}{2}\frac{d}{dt}\int_{\Omega_d} u^2 + \int_{\Omega_d} \nabla u^2 + \alpha\int_{\Omega_d} |\mathbf{v}|^2 = (\gamma R + \alpha)\int_{\Omega_d} v_2 u. \tag{145}$$

Then, we have

$$\frac{1}{2}\frac{d}{dt}\int_{\Omega_d} u^2 \leq 0. \tag{146}$$

whenever

$$\frac{1}{\gamma R + \alpha} \geq \frac{1}{\gamma R^*(\alpha) + \alpha} = \sup \frac{\int_{\Omega_d} v_2 u}{\int_{\Omega_d} \nabla u^2 + \alpha \int_{\Omega_d} |\mathbf{v}|^2}, \tag{147}$$

where the supremo is taken among the admissible functions, i.e., satisfying (i) the regularity requirements of a weak solution of problem (89)-(94), (ii) the homogeneous boundary conditions corresponding to (133)-(136), and (iii) $\operatorname{div}\mathbf{v} = 0$.

Therefore, the stability criterium for solutions of problem (133)-(139) is reduced to solving the maximization problem of the right hand side of (147). We observe that, as in [56], the Euler-Lagrange equations associated to the maximization problem are just the time independent linearized version of (141)-(143), implying that the linear and nonlinear estimates for the bifurcation parameter coincide. We note that the above mentioned differences between the problem treated in [56] and problem (133)-(139) affect to the maximization problem via the set of admissible functions. Indeed, our condition $p = 0$ on $\Gamma_{top} \times (0,T)$ implies that the linear problem to be solved is coupled for the three unknowns and not only for u and $\mathbf{v}$, as in [56].

Assuming periodic behavior in the horizontal variable for the steady state solution of the perturbation problem (141)-(143), namely $u(x,z) = e^{iax}U(z)$, $p(x,z) = e^{iax}P(z)$ and $v_2(x,z) = e^{iax}Q(z)$, we are led to solve the following problem: Find the minimum R^* such that there exist a non-trivial solution $U,P,Q : (d,1) \to \mathbb{R}$ of

$$-U'' + a^2 U = \gamma R^* Q, \quad U(d) = 0, \quad U(1) = 0, \tag{148}$$

$$-P'' + a^2 P = -U', \quad P(d) = 0, \quad P'(1) = 0, \tag{149}$$

$$-Q'' + a^2 Q = a^2 U, \quad Q(d) + P'(d) = 0, \quad P'(1) = 0. \tag{150}$$

Eigenvalue problem (148)-(150) was solved numerically using a standard routine of Mathematica [61]. In Figure 6 we summarize the results concerning to the size of the bifurcation parameter, R^*:

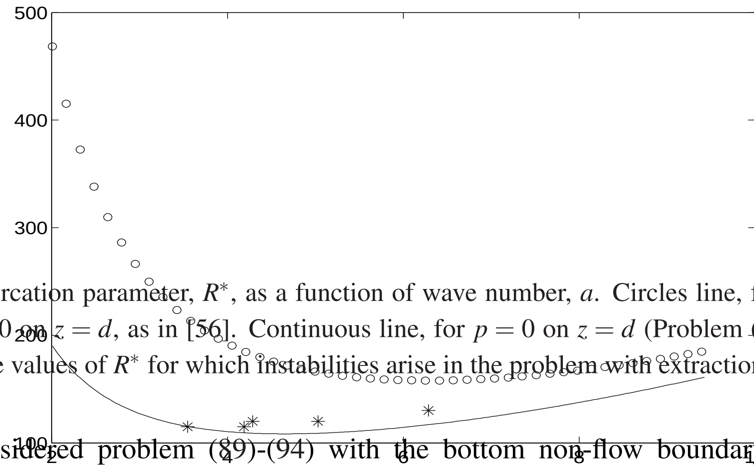

Figure 6. Bifurcation parameter, R^*, as a function of wave number, a. Circles line, for boundary condition $v_2 = 0$ on $z = d$, as in [56]. Continuous line, for $p = 0$ on $z = d$ (Problem (133)-(139)). Asterisks: some values of R^* for which instabilities arise in the problem with extraction.

- We considered problem (89)-(94) with the bottom non-flow boundary condition $\nabla u \cdot \mathbf{n} = 0$ replaced by the Dirichlet boundary condition $u = u^*$, as in (133). In other words, we investigate the importance of the extraction region and the dead core formation for the development of transient instabilities. We computed numerical solutions for parameters values which imply no dead core formation ($u < 1$ on $z = d$), and even in this case we checked the formation of instabilities for values of R which are very close to those of problem (133)-(139). Therefore, the actual formation of a dead core in the extraction region seems not to be relevant for instabilities occurrence as long as the concentration on the bottom boundary keeps lower enough than that on the extraction region.

- We compared the bifurcation curves corresponding to our problem (133)-(139) and to the problem studied in [56], i.e., with our condition $p = 0$ on $z = d$ replaced by $v_2 = 0$ on $z = d$. The non-flow boundary condition seems to give more stability to the system, possibly as a consequence of the shortening of the region in which they may develop.

3.4.1 Numerical simulations

We used a stabilized mixed finite element method in space and implicit finite differences scheme in time to approximate solutions of an equivalent formulation of problem (89)-(94), consisting on combining equations (89) and (90) to replace (89) by

$$u_t + R\mathbf{v} \cdot \nabla u - \Delta u = Rmuf(\cdot, u). \tag{151}$$

It is well known that classical mixed variational formulations need an adequate election of the discrete spaces for the flow and the pressure in order to satisfy the Babuska-Brezzi stability condition, see for instance [15]. Following Masud and Huges [45], we consider a stabilized mixed finite element method for Darcy flows which allows to consider piecewise linear approximations and the same mesh for both pressure and flow. The differences between our problem and the problem treated in [45] are the boundary condition for the pressure and the existence of a source term in (158).

Let $t_n = n\delta t$, for $\delta t = T/N$, and $n = 0, ...N$, and consider the discrete time approximation given by

$$u^n + \delta t(R\mathbf{v}^n \cdot \nabla u^n - \Delta u^n) = \delta t R m u^n f(\cdot, u^n) + u^{n-1}, \tag{152}$$

$$\operatorname{div} \mathbf{v}^n = -mf(\cdot, u^n), \tag{153}$$

$$\mathbf{v}^n = -\nabla p^n - u^n \mathbf{e}_z, \tag{154}$$

in Ω, where the super-index n stands for the approximations in time t_n. The boundary conditions are

$$u^n = u_{top}, \quad p^n = 0 \quad \text{on } \Gamma_{top}, \tag{155}$$

$$\nabla u^n \cdot \mathbf{n} = \mathbf{v}^n \cdot \mathbf{n} = 0 \quad \text{on } \Gamma_N. \tag{156}$$

We solved this nonlinear system of equations by a fixed point method based on the proof of existence of solutions, see Theorem 1. Consider the map $S : L^2(\Omega) \to L^2(\Omega)$ given by $S(\hat{u}; u^{n-1}) = u$, where u is the solution of

$$u - \delta t \Delta u = -\delta t R \mathbf{v} \cdot \nabla \hat{u} + \delta t R m \hat{u} f(\cdot, \hat{u}) + u^{n-1}, \tag{157}$$

$$\operatorname{div} \mathbf{v} = -mf(\cdot, \hat{u}), \tag{158}$$

$$\mathbf{v} = -\nabla p - \hat{u} \mathbf{e}_z, \tag{159}$$

with the mentioned boundary conditions (155)-(156). A fixed point of $S(\cdot\,; u^{n-1})$ is denoted by u^n. The formulation of the stabilized mixed finite element method for problem (158)-(159) is: Find $\mathbf{v} \in H_0(\operatorname{div}, \Omega)$ and $p \in \mathcal{V}$ solutions of

$$\int_\Omega (\mathbf{v} + \nabla p) \cdot \phi = -\int_\Omega \hat{u} \mathbf{e}_z \cdot \phi \quad \text{for all } \phi \in H_0(\operatorname{div}, \Omega), \tag{160}$$

$$\int_\Omega (\nabla p - \mathbf{v}) \cdot \nabla \varphi = -\int_\Omega (\hat{u} \mathbf{e}_z \cdot \nabla \varphi + 2mf\varphi) \quad \text{for all } \varphi \in \mathcal{V}. \tag{161}$$

Once that $\mathbf{v}$ and p are determined, we set the following problem for equation (157): Find $u \in u_{top} + \mathcal{V}$ solution of

$$\int_\Omega u\varphi + \delta t \int_\Omega \nabla u \cdot \nabla \varphi = \delta t R \int_\Omega (m\hat{u} f(\cdot, \hat{u}) - \mathbf{v} \cdot \nabla \hat{u})\varphi + \int_\Omega u^{n-1} \varphi \quad \text{for all } \varphi \in \mathcal{V}. \tag{162}$$

We use the spatial discretization of (160)-(161) given in [45], and adapt it also for equation (162). It consists of finite triangular elements, continuous piecewise linear base functions and the same mesh for all the unknowns. For the practical implementation of the fixed point method, we consider that a discrete solution of (160)-(162) is a fixed point of $S(\cdot\,; u^{n-1})$ if a norm of $S(u_k^n; u^{n-1}) - u_k^n$, for $k = 0, 1, \ldots$, with $u_0^n = u^{n-1}$, is smaller than a fixed tolerance.

For the numerical simulations, we considered the spatial domains $\Omega = (0,1) \times (0,1)$ and $\Omega_d = (0,1) \times (0.25,1)$, i.e., the extraction zone is above $z = 0.25$, and the initial and

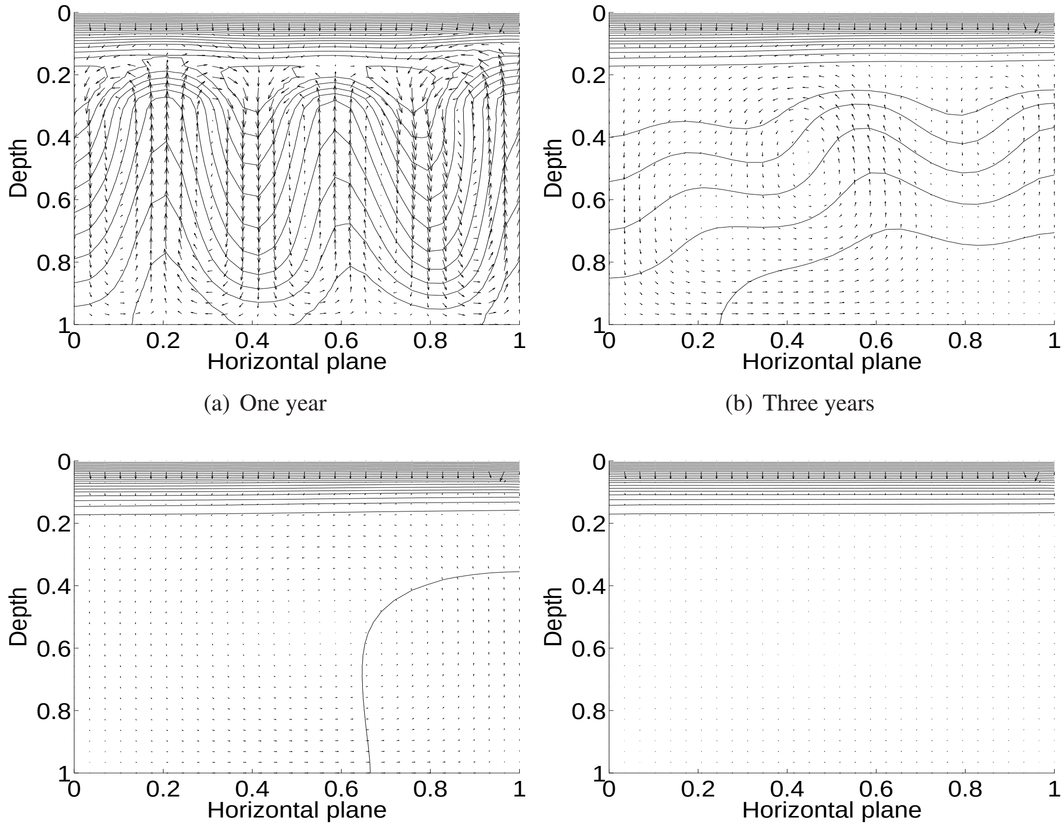

(a) One year

(b) Three years

(c) Seven years

(d) Twelve years

Figure 7. Flow and contour lines of the salt concentration for the solution of problem (89)-(93) with parameters $u_0 = u_D = 0.5$, $R = 1400$, $m = 0.07$, $r = 1$, $d = 0.25$.

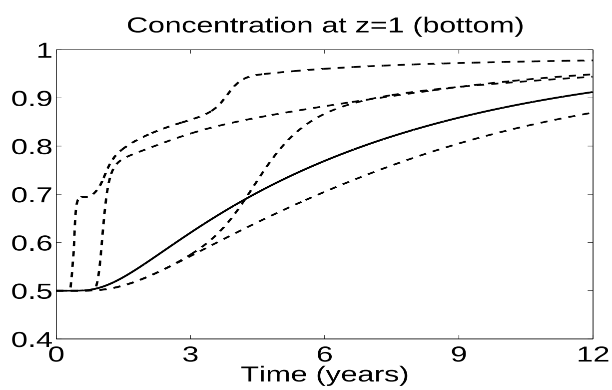

Figure 8. Time evolution of salt concentration at the bottom boundary, $z = 1$. Continuous line: solution of the 1-D model for $m_1 = Rm = 98$. Dotted lines: x-averaged solutions of the 2-D model, see (163), for $R = 140,\ 200,\ 500,\ 1400$ and corresponding m's such that $Rm = 98$. Concentrations are ordered increasingly according to the value of R. Transient instabilities are reflected in the steep increase of the concentration of the 2-D model for high R. $u_0 = u_D = 0.5$, $r = 1$.

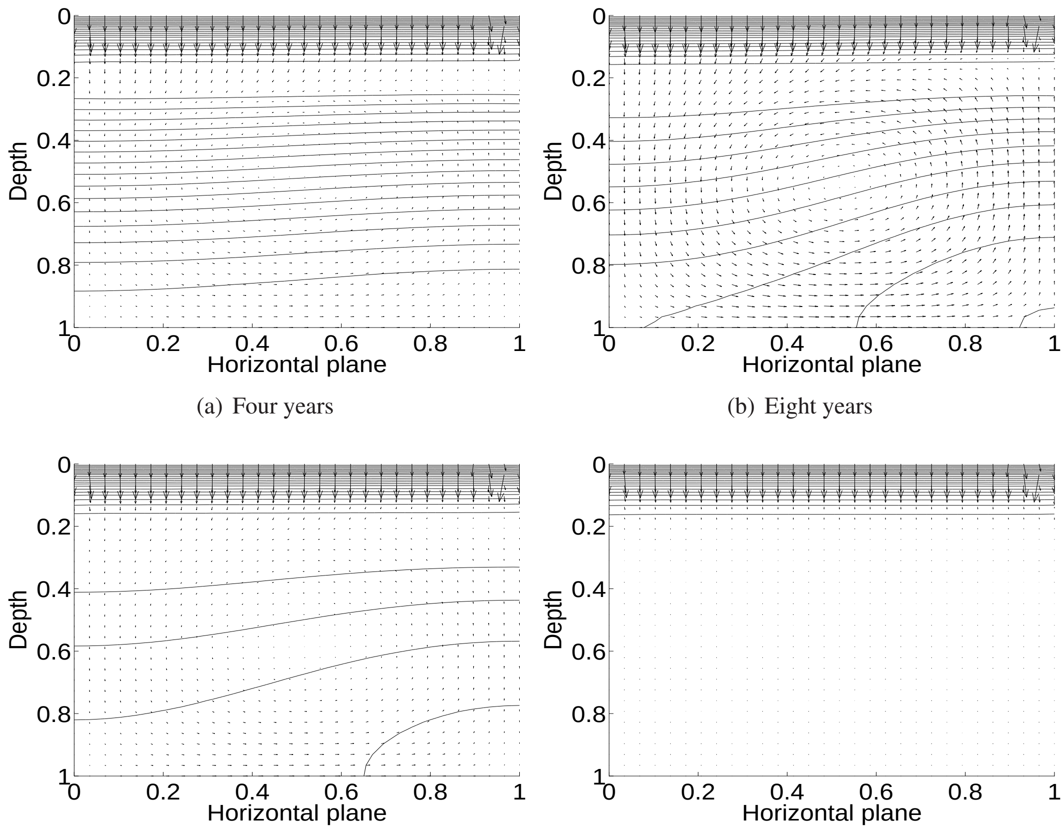

(a) Four years

(b) Eight years

(c) Fourteen years

(d) Twenty four years

Figure 9. Flow and contour lines of salt concentration for the solution of problem (89)-(93) with parameters $u_0 = u_D = 0.5$, $R = 140$, $m = 0.7$, $r = 1$, $d = 0.25$.

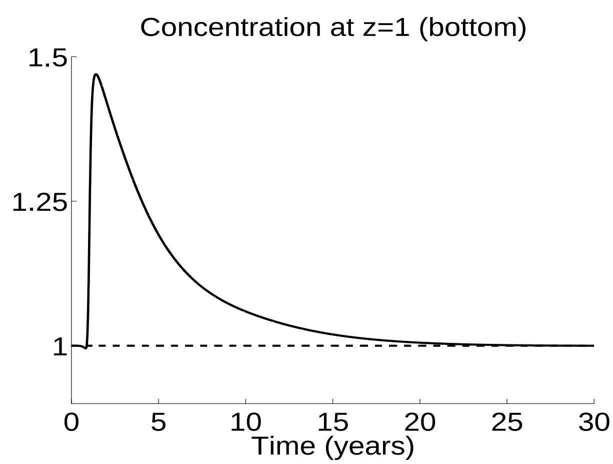

Figure 10. Time evolution of the concentration ratio (see (164)) at the bottom boundary, $z = 1$, for $R = 500$ and $m = 0.196$ ($m_1 = Rm = 98$). Transient instabilities speeds up the salt mixing and increase the salt concentration. However, the long time behavior is the same for solutions of the 1-D and 2-D models. $u_0 = u_D = 0.5$, $r = 1$.

top boundary data to be constant, $u_{top} = u_0 = 0.5$. We used an uniform triangular mesh with 900 triangles and an initial time step of $\delta t = 1/20R$. The time step is adapted according to the size of $\|u^n - u^{n-1}\|$. We tested several values for the power, r, lower and equal to one, in particular, values for which a dead core arises. However, the occurrence of transient instabilities seems to be independent of this choice so we only plot the results corresponding to $r = 1$. In order to compare with the 1-D solution, we chose several sets of values for R and m such that the product $m_1 = Rm$ keeps constant and equal to 98, a relatively mild physical situation.

In Figures 7 and 9, flow and concentration contour lines are plotted.

(a) Figure 7. Flow and concentration contour lines for a high Rayleigh number, $R = 1400$, and a small extraction number, $m = 0.07$. Large and strong Bérnard type instability cells arises in an early transient estate (one year) producing a rapid mix of the salt content. Instabilities decrease with time and after a computed time of seven years, the system is practically stable.

(b) Figure 9. Flow and concentration contour lines for a small Rayleigh number, $R = 140$, and extraction number, $m = 0.7$. It takes longer for the formation of instabilities, which are also weaker.

(c) Figure 8. We plot the salt concentration of the 1-D solution at $z = 1$, i.e, $u_1(1,t)$, and the mean salt concentration at $z = 1$ of the 2-D solution, i.e.

$$\frac{1}{L}\int_0^L u_2(x,t,1)dx, \tag{163}$$

where u_1 and u_2 are the one and two-dimensional solutions, respectively, of problem (89)-(94), for several values of R and m such that $m_1 = Rm$, where m_1 is the only parameter appearing in the 1-D model, see (95). These values are

$$(R,m) = \{(140,\ 0.7),(200,\ 0.49),(500,\ 0.196),(1400,\ 0.07)\}.$$

We check that instabilities accelerates the mixing and the approach to the steady state. For $R = 200$ instabilities takes time to appear (about three years) and when it occurs, they are persistent on time (till year six) but not very strong, as may be observed in the concentration slope. For $R = 500$ instabilities appear sooner (year one), with much strength (large slope) but decay rapidly. The plot for the solution corresponding to a high Rayleigh number, $R = 1400$ is more complex. Instabilities appear almost immediately and with great strength. Afterwords, the mixing seems to moderate for a short period, after which a new rapid increase of the salt concentration takes place. At year two, a new period of moderate increase starts, but is again broken at about year four, when a new rapid increase happens. After that, the system seems to stabilize. Finally, for smaller values of R, the behavior of the 2-D solution is similar to the 1-D case. However, the mean value of u_2 on $z = 1$ is smaller than $u_1(1,\cdot)$ for all plotted times, probably as a result of the energy consumption in weak instabilities and the difficulties for flow circulation at the corners.

(d) Figure 10. We compare the speed of approach to the steady state between the one and the two-dimensional solutions of problem (89)-(94) when instabilities in the transient state are present ($R = 500$). We plot, against time, the ratio

$$\frac{1}{Lu_1(1,t)} \int_0^L u_2(x,1,t)dx, \tag{164}$$

where u_1 and u_2 are the one and two-dimensional solutions, respectively, of problem (89)-(94). We observe three time intervals with different behaviors of this ratio. Initially, when instabilities did not develop yet, both solutions are practically equal. Afterwards, when instabilities appear, the mixing in the two-dimensional model is accelerated and the increase of the solute concentration, u_2, at the bottom boundary is up to the fifty per cent greater than the corresponding one-dimensional solution, u_1. Finally, for later times, this ratio decreases and slowly approaches to one, indicating that the stationary states are the same for both problems.

4 The water-soil one-dimensional model in stagnant water conditions

In this section we present a simplified water-soil model which tries to capture the situation in which water is stagnant and, therefore, mangroves, while extracting the available water form the reservoir, also salinize it. The problem is formulated, as before, in terms of the coupled system of partial differential equations for the salt concentration and the water flow in the porous medium given in (96)-(97), but with a different boundary condition on the top of the soil, i.e., on the interface connecting both subdomains.

The main mathematical difficulty of this model when compared with those studied in Section 3 is that the closure of water income to the natural system and hence the balance equations for salt and water content lead to a *dynamical boundary condition* at such interface, i.e., a boundary condition involving the time derivative of the solution. Although not too widely considered in the literature, dynamic boundary conditions date back at least to 1901 in the context of heat transfer [49]. Since then, they have been studied in many applied investigations in several disciplines like Stefan problems [51, 55], fluid dynamics [28], diffusion in porous medium [27], mathematical biology [26] or semiconductor devices [53]. From a more abstract point of view the reader is referenced to, among others, [10, 17, 25, 37, 43].

Apart from the mathematical technical details, one of the main features of the dynamic boundary condition when compared to the Dirichlet boundary condition is the elimination of the boundary layer the latter creates in a neighborhood of the water-soil interface, layer in which the salt concentration keeps well below the threshold salinity level. Thus, this new model allows us to describe the situation in which a continuous increase of fresh water uptake by the roots of mangroves drives the ecosystem to a complete salinization.

4.1 Derivation of the model

In the porous medium domain, we consider the same equations and lateral and bottom boundary conditions than in problem (96)-(99) for the rescaled dimensionless unknowns

u_D and v_D. The mathematical difference between both model arises in the interface condition between soil and water. On this interface we prescribe a boundary condition which is deduced from conservation laws for salt and water in the whole system water-soil. We assume that salt concentration in the water domain, u_S, remains uniformly distributed in space. This approximation is justified when assuming a faster mixing of the salt in the reservoir than in the porous medium. Then, the average height level of the water reservoir, W, and the salt concentration in the water domain, u_S, are functions that only depend on time. We further consider, based on a continuity assumption,

$$u_S(t) = u_D(0,t) \quad \text{for } t \in (0,T). \tag{165}$$

We have:

- The salt balance. Assuming that the total amount of salt in the system water-soil remains constant, we have

$$\frac{d}{dt}\big(u_S w + \int_0^1 u_D\big) = 0 \quad \text{in } (0,T),$$

  with $w = W/\theta H$, the dimensionless reservoir height. Therefore, from equation (96) (with u replaced by u_D) and the bottom boundary conditions in (98),

$$\frac{d(u_S w)}{dt} = u_D(0,\cdot)v_D(0,\cdot) - u_{D,z}(0,\cdot) \quad \text{in } (0,T). \tag{166}$$

- The fluid balance, which asserts that the amount of water taken up from the soil by the roots of mangroves is replaced by water from the reservoir:

$$\frac{dw}{dt} = -v_D(0,\cdot) \quad \text{in } (0,T). \tag{167}$$

Combining (165)-(167) we deduce

$$w(t)u_{D,t}(0,t) = u_{D,z}(0,t) \quad \text{for } t \in (0,T), \tag{168}$$

which is the dynamic boundary condition for the soil-water interface.

We are led then to the following problem for $u = u_D$, $v = v_D$ and w in $Q_T = (0,1) \times (0,T)$: Find $u : \bar{Q}_T \to [0,1]$, $v : \bar{Q}_T \to \mathbb{R}$ and $w : [0,T] \to \mathbb{R}$ such that

$$u_t + (uv - u_z)_z = 0, \tag{169}$$

$$v_z + m_1 f(\cdot,u) = 0 \quad \text{in } Q_T = \Omega \times (0,T), \text{ with } \Omega = (0,1), \tag{170}$$

$$w'(t) + v(0,t) = 0 \quad \text{for } t \in (0,T), \tag{171}$$

subject to the boundary and initial conditions

$$w(t)u_t(0,t) = u_z(0,t), \tag{172}$$

$$u_z(1,t) = v(1,t) = 0 \qquad \text{for } t \in (0,T), \tag{173}$$

$$u(\cdot,0) = u_0 \quad \text{in } \Omega, \qquad w(0) = w_0. \tag{174}$$

We assume Hypothesis H_2 (see page 14) on function f while H_3 and H_4 are replaced by

H_3'. The initial data posses the regularity

$$u_0 \in H^1(\Omega) \quad \text{with } 0 \leq u_0 \leq 1 \quad \text{in } \Omega.$$

H_4'. The function w is a positive constant. The number m is positive.

Remark 4 The assumption w constant in H_4' has a reasonable range of validity. Integrating (171) in $(0,t)$ and using (170) we obtain, for f of the usual type (22)

$$w(t) = w_0 - \frac{m_1}{d} \int_0^t \int_0^d (1 - u(z,\tau))^r dz d\tau.$$

Using property (175) below for an increasing sequence of *initial data* as $u_0 \in \{0.5, 0.75, 0.9, 0.99\}$ and $r = 1$ we find for the dimensional variables

$$W(t) - W_0 \geq -\tau_0 t \{0.5, 0.25, 0.1, 0.01\}.$$

Taking $\tau_0 \approx 10^{-8}\,\mathrm{m\,s^{-1}}$ and $t \approx 1\,$year, this means that the reservoir will decrease about, respectively, $\{0.15, 0.075, 0.03, 0.003\}$ meters per year. Therefore, the assumption of small variation in the reservoir height seems reasonable, specially once that the salt concentration has raised sufficiently.

4.2 Existence of solutions and other qualitative results

We prove the following result on existence and regularity of solutions.

Theorem 5 *Assume H_2, H_3' and H_4'. There exists a strong solution of problem (169)-(174), defined as*

1. *For any* $\alpha \in (0,\infty)$,

$$u \in W^{1,\alpha}(0,T;L^\alpha(\Omega)) \cap L^\alpha(0,T;W^{2,\alpha}(\Omega)) \cap C((0,T];C(\bar{\Omega})),$$
$$v \in C((0,T];\mathcal{W})$$

   with $\mathcal{W} := \left\{\varphi \in W^{1,\infty}(\Omega) : \varphi(1) = 0\right\}$.

2. *The differential equations (169) and (170) and the boundary conditions (172) and (173) are satisfied almost everywhere.*
3. *The initial distribution is satisfied in the sense*

$$\lim_{t\to 0} \|u(\cdot,t) - u_0\|_{L^2(\Omega)} = 0.$$

In addition, u satisfies

$$u \geq u_m := \min_{\bar{\Omega}} u_0 \quad \text{a.e. in } Q_T, \tag{175}$$

and, if for some $\beta > 0$

$$f \in C^\beta(\bar{\Omega} \times [0,1]) \quad \text{and} \quad u_0 \in C^{2+\beta}(\bar{\Omega}), \tag{176}$$

and u_0 satisfies the compatibility condition

$$u_0'(0)+u_0'(0)\int_0^1 m_1 f(x,u_0(x))dx - u_0''(0) = m_1 f(0,u_0(0))u_0(0), \tag{177}$$

then $u\in C^{1+\beta,2+\beta}(\bar{Q}_T)$ and $v\in C^{1+\beta,1+\beta}(\bar{Q}_T)$.

Similar qualitative properties to those proven for problem (96)-(99), with Dirichlet boundary conditions at the top boundary, may be proven for problem (169)-(174). In particular, uniqueness of solutions holds under the same assumptions than in Theorem 3. However, one important effect of the dynamic boundary condition when compared to the Dirichlet boundary condition is the elimination of the boundary layer at the top boundary. As a consequence, the unique solution of the steady state problem corresponding to problem (169)-(174), i.e., functions $U\in H^1(\Omega)$ and $V\in\mathcal{W}$ satisfying

$$\begin{aligned}&(VU-U_z)_z=0,\quad V_z+m_1 f(\cdot,U)=0 \quad \text{in } \Omega,\\ &U_z(0)=U_z(1)=0,\end{aligned}$$

is the trivial solution $(U,V)=(1,0)$. Regarding the asymptotic convergence of solutions of problem (169)-(174) to this trivial solution when $t\to\infty$, we have the following result, see [30] for the proof.

Theorem 6 *Assume H_1-H_3 and $\min_{\bar{\Omega}} u_0>0$, and let (u,v) be a strong solution of problem (169)-(174). Then*

$$(u,v)\to(1,0) \quad \text{in } L^2(\Omega) \quad \text{and} \quad u(0,t)\to 1 \quad \text{pointwise} \quad \text{as } t\to\infty.$$

Proof of Theorem 5. Without loss of generality, we set $m_1=w=1$ for clarity. We first prove the existence of weak solution of a time discretization of problem (169)-(174). Since, a priori, the component u of solutions to approximated problems will not necessarily satisfy $0\le u\le 1$, we extend f by $\bar{f}$ as $\bar{f}(x,\sigma)=0$ if $\sigma>1$, $\bar{f}(x,\sigma)=f(x,\sigma)$ if $0\le\sigma\le 1$ and $\bar{f}(x,\sigma)=f(x,0)$ if $\sigma<0$. We denote the corresponding problem by Problem $\bar{\text{P}}$.

Lemma 4 *For $\tilde{u}\in H^1(\Omega)$, and $\tau>0$ small enough, there exists a solution $(u,v)\in W^{2,\alpha}(\Omega)\times\mathcal{W}$, with $\alpha<\infty$, of*

$$u+\tau(uv-u_z)_z=\tilde{u} \quad \text{a.e. in } \Omega, \tag{178}$$

$$v_z+\bar{f}(\cdot,u)=0 \quad \text{a.e. in } \Omega, \tag{179}$$

$$u(0)=\tilde{u}(0)+\tau u_z(0), \quad u_z(1)=0. \tag{180}$$

Proof. We introduce the set $K=\left\{v\in\mathcal{W}, \|v\|_{W^{1,\infty}}\le\rho\right\}$, for some $\rho>0$ to be fixed. It is clear that K is convex and weakly compact in the star topology of $W^{1,\infty}(\Omega)$. For $\hat{v}\in K$, we define the map

$$S(\hat{v})(z):=\int_z^1 \bar{f}(s,u(s))ds,$$

with $u \in H^1(\Omega)$ solution of

$$\int_\Omega (u-\tilde{u})\varphi + \tau \int_\Omega u_z \varphi_z + \tau \int_\Omega (u\hat{v})_z \varphi + (u(0)-\tilde{u}(0))\varphi(0) = 0, \tag{181}$$

for any $\varphi \in H^1(\Omega)$. The existence of a unique solution of (181) is guaranteed by the Theorem of Lax-Milgram (see, for instance, [14]). In addition, we have

$$\|u_{zz}\|_{L^2} \leq \frac{1}{\tau}\|u-\tilde{u}\|_{L^2} + \|u\|_{L^2}\|\bar{f}\|_{L^\infty} + \|u_z\|_{L^2}\|v\|_{L^\infty}, \tag{182}$$

i.e., $u \in H^2(\Omega)$. Since $\tilde{u} \in H^1(\Omega) \subset C(\bar{\Omega})$, a boot-strap argument allows us to deduce $u \in W^{2,\alpha}(\Omega)$, for any $\alpha < \infty$. A standard argument allows us to conclude that u satisfies (178) and (180) (with $\hat{v}$ replaced by v).

Observe that a fixed point of S is a solution of (178)-(180). We prove the existence of such a fixed point using a theorem by [6], for which we need to show: (i) $S(K) \subset K$ and (ii) S is weakly-weakly continuous in the star topology of $W^{1,\infty}(\Omega)$. Showing $S(K) \subset K$ is straightforward since for any $\hat{v} \in K$, $\|S(\hat{v})\|_{W^{1,\infty}} \leq 2\|\bar{f}\|_{L^\infty} =: \rho$.

To prove the weak continuity, (ii), we consider a sequence $\hat{v}_j$ and a function $\hat{v}$ in K such that $\hat{v}_j \to \hat{v}$ weakly star in $W^{1,\infty}(\Omega)$. Let u_j and u be the corresponding solutions of problem (181). Taking $\varphi = u_j$ in (181) we obtain, after using Schwarz's inequality,

$$u_j(0)^2 + (1 - \tau\|\hat{v}_j\|^2_{L^\infty} - 2\tau\|\hat{v}_{jz}\|_{L^\infty})\|u_j\|^2_{L^2} + \tau\|u_{jz}\|^2_{L^2} \leq \|\tilde{u}\|^2_{L^2} + \tilde{u}(0)^2.$$

For τ small enough and independent of j we get $E_j + \tau\|u_{jz}\|^2_{L^2} \leq c$, with c independent of τ and j, and with

$$E_j = u_j(0)^2 + \|u_j\|^2_{L^2}. \tag{183}$$

Therefore, we obtained a uniform bound which allows us to extract a subsequence of u_j (not relabelled) such that $u_j \to u^*$ weakly in $H^1(\Omega)$, for some $u^* \in H^1(\Omega)$. Since the embedding $H^1(\Omega) \subset C(\bar{\Omega})$ is compact, extracting a new subsequence if necessary we have $u_j \to u^*$ uniformly in $C(\bar{\Omega})$. Next we show that, actually, $u^* = u$. All the terms in (181) corresponding to $(u_j, \hat{v}_j)$ are well defined in the limit $j \to \infty$. For instance,

$$\int_\Omega (u_j \hat{v}_j)_z \varphi = \int_\Omega u_{jz}\hat{v}_j \varphi + \int_\Omega u_j \hat{v}_{jz}\varphi \to \int_\Omega (u^*\hat{v})_z \varphi,$$

due to the convergences $u_j \to u$ weakly in $H^1(\Omega)$ and uniformly in $C(\bar{\Omega})$, and $\hat{v}_j \to \hat{v}$ weakly star in $W^{1,\infty}(\Omega)$ and uniformly in $C(\bar{\Omega})$ (by compact embedding, again). Then, by the uniqueness of solution of problem (181) we deduce $u^* = u$. Hence,

$$S(\hat{v}_j)(z) = \int_z^1 \bar{f}(s, u_j(s))ds \to \int_z^1 \bar{f}(s, u(s))ds = S(\hat{v})(z),$$

uniformly in $C^1(\bar{\Omega})$ and, in particular, weakly star in $W^{1,\infty}(\Omega)$. Therefore, (ii) is proven and the existence of a fixed point deduced. □

We now construct piecewise constant in time approximations of solutions of Problem $\bar{\mathrm{P}}$. Let $(0,T] = \bigcup_{k=1}^K ((k-1)\tau, k\tau]$, with $\tau = T/K$ and $K \in \mathbb{N}$. For $k = 1,\dots,K$, define recursively (u_k, v_k) as the solution of problem (178)-(180) with $\tilde{u} = u_{k-1}$, $u = u_k$ and $v = v_k$.

Let the initialization of this recursion be the initial data of Problem $\bar{\mathrm{P}}$, u_0. We define the following piecewise constant in time functions: $u^{(\tau)}(z,t) = u_k(z)$, $v^{(\tau)}(z,t) = v_k(z)$,

$$\partial_t^{(\tau)} u^{(\tau)}(z,t) = \frac{u_k(z) - u_{k-1}(z)}{\tau}, \quad E^{(\tau)}(t) = \frac{1}{2}\big(|u^{(\tau)}(0,t)|^2 + \int_\Omega |u^{(\tau)}|^2\big),$$

if $z \in \Omega$, $t \in ((k-1)\tau, k\tau]$, for $k = 1, \ldots, K$.

Lemma 5 *As $\tau \to 0$ there exist a subsequence of $(u^{(\tau)}, v^{(\tau)})$ (not relabelled) such that*

$$u^{(\tau)} \to u \quad \text{weakly star-weakly in } L^\infty(0,T;H^1(\Omega)), \tag{184}$$
$$\partial_t^{(\tau)} u^{(\tau)} \to \partial_t u \quad \text{weakly in } L^2(Q_T), \tag{185}$$
$$\partial_t^{(\tau)} u^{(\tau)}(0,\cdot) \to \partial_t u(0,\cdot) \quad \text{weakly in } L^2(0,T), \tag{186}$$
$$u^{(\tau)} \to u \quad \text{weakly in } L^2(0,T;H^2(\Omega)), \tag{187}$$
$$u^{(\tau)} \to u \quad \text{uniformly in } C((0,T];C(\bar{\Omega})), \tag{188}$$
$$v^{(\tau)} \to v \quad \text{uniformly-strongly in } C((0,T];\mathcal{W}). \tag{189}$$

Proof. Replacing in (178) functions u, v and $\tilde{u}$ by u_k, v_k and u_{k-1}, respectively, and using $\varphi = u_k$ in the weak formulation (181) (with $\hat{v} = v$) , we obtain, after using the inequalities of Schwarz and $x(x-y) \geq (x^2 - y^2)/2$,

$$E_k + \tau \|u_{kz}\|_{L^2}^2 \leq E_{k-1} + \tau c_f E_k,$$

for

$$E_k = \frac{1}{2}\big(u_k(0)^2 + \int_\Omega u_k^2\big),$$

and with $c_f := \|\bar{f}\|_{L^\infty}^2 + \|\bar{f}\|_{L^\infty}$. Then, from the Gronwall's discrete inequality and $k\tau \leq K$, we deduce $E_k \leq cE_0$, for $k = 1, \ldots, K$, and for some constant, c, independent of τ. Therefore,

$$\frac{E_k - E_{k-1}}{\tau} + \|u_{kz}\|_{L^2}^2 \leq cc_f E_0.$$

Integrating in $(0,t)$, for any $t \in (0,T)$, we obtain

$$E^{(\tau)}(t) + \int_{Q_t} |u_z^{(\tau)}|^2 \leq cc_f E_0,$$

which gives a uniform estimate for $u^{(\tau)}$ in the norm of $L^2(0,T;H^1(\Omega)) \cap L^\infty(0,T;L^2(\Omega))$. On the other hand, from (179) we obtain $\|v_k\|_{W^{1,\infty}} \leq \|\bar{f}\|_{L^\infty}$, which implies the uniform bound

$$\|v^{(\tau)}\|_{L^\infty(W^{1,\infty})} \leq \|\bar{f}\|_{L^\infty}.$$

We now choose $\varphi = (u_k - u_{k-1})/\tau$ in (181) (with $\hat{v} = v$). We get

$$\int_\Omega \Big|\frac{u_k - u_{k-1}}{\tau}\Big|^2 + \int_\Omega u_{kz}\Big(\frac{u_k - u_{k-1}}{\tau}\Big)_z + \int_\Omega (u_k v_k)_z \frac{u_k - u_{k-1}}{\tau} + \Big|\frac{u_k(0) - u_{k-1}(0)}{\tau}\Big|^2 = 0.$$

Using again the inequality $x(x-y) \geq (x^2 - y^2)/2$, we obtain

$$\int_\Omega u_{kz}\Big(\frac{u_k - u_{k-1}}{\tau}\Big)_z \geq \frac{1}{2\tau}\int_\Omega (|u_{kz}|^2 - |u_{(k-1)z}|^2),$$

and therefore

$$\int_\Omega |\frac{u_k - u_{k-1}}{\tau}|^2 + \frac{1}{2\tau}\int_\Omega (|u_{kz}|^2 - |u_{(k-1)z}|^2) + \int_\Omega (u_k v_k)_z \frac{u_k - u_{k-1}}{\tau} + |\frac{u_k(0) - u_{k-1}(0)}{\tau}|^2 \leq 0.$$

Integrating in $((k-1)\tau, k\tau)$ and adding from $k=1$ to K leads to

$$\frac{1}{2}\int_\Omega |u_z^{(\tau)}|^2(T,\cdot) + \int_{Q_T} |\partial_t^{(\tau)} u^{(\tau)}|^2 + \int_0^T |\partial_t^{(\tau)} u^{(\tau)}(0,\cdot)|^2 \leq \frac{1}{2}\int_\Omega |u_{0z}|^2 - \int_{Q_T} (u^{(\tau)} v^{(\tau)})_z \partial_t^{(\tau)} u^{(\tau)}.$$

Using Hölder's inequality we deduce

$$\|u_z^{(\tau)}\|^2_{L^\infty(L^2)} + \|\partial_t^{(\tau)} u^{(\tau)}\|^2_{L^2(L^2)} + \|\partial_t^{(\tau)} u^{(\tau)}(0,\cdot)\|^2_{L^2(0,T)} \leq c\big(\|u_0\|^2_{H^1} + \|v^{(\tau)}\|^2_{W^{1,\infty}} \|u^{(\tau)}\|^2_{L^2(H^1)}\big),$$

i.e., additional uniform bounds for

$$\begin{aligned} &u^{(\tau)} && \text{in } L^\infty(0,T;H^1(\Omega)), \\ &\partial_t^{(\tau)} u^{(\tau)} && \text{in } L^2(Q_T), \qquad (190)\\ &\partial_t^{(\tau)} u^{(\tau)}(0,\cdot) && \text{in } L^2(0,T). \qquad (191) \end{aligned}$$

Once we have the uniform bound on the time derivative, (190), we deduce from (182) a uniform bound for $u^{(\tau)}$ in $L^2(0,T;H^2(\Omega))$, i.e. (187). Therefore, there exist $u \in L^\infty(0,T;H^1(\Omega)) \cap H^1(0,T;L^2(\Omega))$ and $v \in L^\infty(0,T;\mathcal{W})$ such that (184) and (185) hold. I addition, the compactness result of [54] implies (188). Therefore, since $\bar{f} \in L^\infty(\Omega;C(\mathbb{R}))$ we have $v_z^{(\tau)} = \bar{f}(\cdot,u^{(\tau)}) \to \bar{f}(\cdot,u) = v_z$ uniformly-strongly in $C((0,T];L^\infty(\Omega))$, and then (189). Finally, from (191) we deduce (186). □

End of proof of Theorem 5
We are now ready to pass to the limit $\tau \to 0$. The pair $(u^{(\tau)}, v^{(\tau)})$ satisfies

$$\int_{Q_T} \partial_t^{(\tau)} u^{(\tau)} \xi + \int_{Q_T} u_z^{(\tau)} \xi_z + \int_{Q_T} (u^{(\tau)} v^{(\tau)})_z \xi + \int_0^T \partial_t^{(\tau)} u^{(\tau)}(0,\cdot)\xi(0,\cdot) = 0, \qquad (192)$$

for $\xi \in L^2(0,T;H^1(\Omega))$, and

$$v_z^{(\tau)} + \bar{f}(\cdot,u^{(\tau)}) = 0 \quad \text{a.e. in } Q_T, \quad v^{(\tau)}(1,t) = 0 \quad \text{for all } t \in (0,T]. \qquad (193)$$

Taking the limit $\tau \to 0$ in (192)-(193), and using (184)-(189) we obtain that (u,v) satisfies

$$\int_{Q_T} u_t \xi + \int_{Q_T} u_z \xi_z + \int_{Q_T} (uv)_z \xi + \int_0^T u_t(0,\cdot)\xi(0,\cdot) = 0, \qquad (194)$$

and

$$v_z + \bar{f}(\cdot,u) = 0 \quad \text{a.e. in } Q_T, \quad \text{and } v(1,t) = 0, \quad \text{for all } t \in (0,T].$$

Due to (187) we deduce $u_{zz} \in L^2(Q_T)$. Integrating by parts in (194) and using $\bar{f} \in L^\infty(\Omega, C(\mathbb{R}))$, we deduce that (u,v) satisfies the strong formulation (169)-(174) and it is, therefore, a strong solution of Problem $\bar{\mathrm{P}}$.

Finally, using $\xi := \min\{0, u-\gamma\}$, with $\gamma = \min_{\bar{\Omega}} u_0$, and $\xi := \max\{0, u-1\}$ as test functions in (194) one easily shows that $\gamma \le u \le 1$ in $\bar{Q}_T$. We note at this point that this property implies $\bar{f}(\cdot,u) = f(\cdot,u)$ in $\bar{Q}_T$ and therefore the pair (u,v) is also a strong solution of problem (169)-(174).

Finally, if function f and the initial condition satisfy the additional regularity and compatibility conditions stated in Theorem 5 then $u \in C(\bar{Q}_T)$ which implies $uf(\cdot,u), v_z \in C^\beta(\bar{Q}_T)$ and, therefore, $u_t - u_{zz} \in C^\beta(\bar{Q}_T)$, implying the additional regularity assertion. □

4.3 Numerical examples

For the numerical solution of problem (169)-(174) we considered, as for the problem with Dirichlet data, an equivalent non-local formulation. It reads

$$u_t + m_1\left(u\int_z^1 f(\cdot,u)\right)_z - u_{zz} = 0 \quad \text{in } Q_T, \tag{195}$$

$$w'(t) = -m_1\int_0^1 f(z,u(z,t))dz \quad \text{for } 0<t<T, \tag{196}$$

$$w(t)u_t(0,t) = u_z(0,t), \quad u_z(1,t) = 0 \quad \text{for } 0<t<T, \tag{197}$$

$$u(\cdot,0) = u_0 \quad \text{in } \Omega. \tag{198}$$

Although till now we have worked under Hypothesys H_4', i.e., that the level height of the reservoir changes relatively slow ($w = const.$), we perform the numerical experiments also for the case in which w is variable, in order to compare the results with the constant case.

To compute approximate solutions we employed the following explicit finite difference scheme

$$u^{\tau+1} = u^\tau + \tau\big(u_{zz}^\tau + m_1 u^\tau f(\cdot,u^\tau) - m_1 u_z^\tau \int_z^1 f(\cdot,u^\tau)\big), \tag{199}$$

$$w^{\tau+1} = w^\tau - m_1\int_0^1 f(z,u^\tau(z))dz, \tag{200}$$

$$u^{\tau+1}(0) = u^\tau(0) + \frac{\tau}{w^\tau}u_z^\tau(0), \quad u^{\tau+1}(1) = 0, \tag{201}$$

$$u^0 = u_0. \tag{202}$$

When we assume H_4', we only solve equations (199), (201) and (202), with $w^\tau = const$. Observe that for solving the whole system it is necessary to have $w^\tau > 0$, due to the dynamic boundary condition in (200).

Parameters are fixed as in the steady state and evolution Dirichlet boundary condition problems, see page 26. We run eight numerical experiments (for both w constant and variable) corresponding to the data shown in Table 4, which coincides with those of Experiments 1, 2, 5 and 6 for the Dirichlet boundary data problem, see page 26. Whenever w is variable and unknown, we set its initial data as $w(0) = 10$, corresponding to a dimensional height $W(0) = \theta H w \approx 5$ m. When w is constant we just take $w = 10$.

Table 4. Data for numerical experiments

Experiment	1	2	3	4
u_0	0.25	0.25	0.50	0.25
m_1	20	20	20	200
r	1	0.5	1	1

In Figures 11 and 13 we show the results on salt concentration for Experiments 1-4, for variable and fixed w, respectively. As a first observation, we note that the problem with fixed height reservoir takes longer to reach the steady state than the problem with variable height and also with those having prescribed Dirichlet boundary data at the top, see Figures 4 and 5. This is motivated by the slower increasing of the salt concentration on the top, $u(0,t)$, as may be seen in Figure 12, where we show the evolution in time of the salt concentration at the top boundary for the eight experiments. The mathematical explanation is the following. From equation (196) we get

$$w(t) = w(0) - m_1 \int_\Omega f(z,u(z,t))dz < w(0) \quad \text{for all} \quad t > 0.$$

Then, from equation (197) and the observation of $u_z(0,t) > 0$, we obtain

$$u_t(0,t) = \frac{1}{w(t)} u_z(0,t) > \frac{1}{w(0)} u_z(0,t),$$

which shows why the salt concentration on the top is alway greater for the variable height problem.

In Figure 12, Plot (a), we also see that a large extraction number produces a faster increase in salt concentration at the top boundary, almost reaching the threshold value in 15 years. It is also interesting the comparison between Experiments 2 and 3, for which we observe that a smaller power r in the extraction function (Experiment 2) compensates the lower initial data and overcomes the salt concentration on the top of Experiment 3 after 30 years. However, this is not the case for the fixed height problem, Plot (b) of the same figure, probably due to the slower velocity of the whole process.

In Figure 14 (a) we show the evolution in time of the height reservoir for the experiments with variable w. For Experiments 4 and 2, we see that a strong extraction due to either a high extraction number or a low power r combined with a low initial salt concentration leads to a fast and intense draining of the reservoir. Solution of the Experiment 1 takes longer for the water extraction but seems to converge to a similar value. Only the solution of Experiment 3, with a higher initial salt concentration, keeps the water level above 50% after 40 years. However the effect of the water level decrease on the salt concentration seems to be not very drastic. Finally, in Figure 14 (b) we show the evolution in time of the relative error

$$\frac{\|u_1(\cdot,t) - u_2(\cdot,t)\|_{L^2(\Omega)}}{\|u_1(\cdot,t)\|_{L^2(\Omega)}}, \tag{203}$$

where u_1 and u_2 are the solutions corresponding to constant and variable w, respectively, for the four sets of data. As we see, all the experiments have an error below 10% during the first twenty years, and Experiments 2, 3 and 4 keep this bound during the forty years analyzed. Remarkably, for Experiment 3 the error is always below 2.5%.

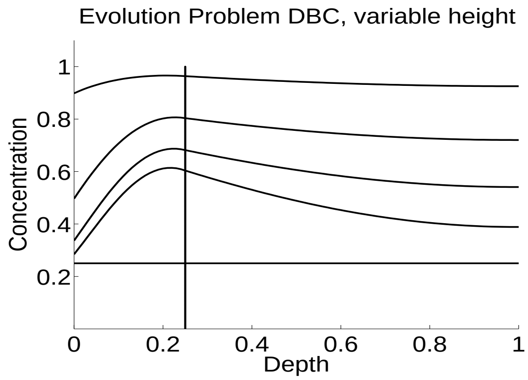

(a) Experiment (1) $u_0 = 0.25$, $m_1 = 20$ and $r = 1$.

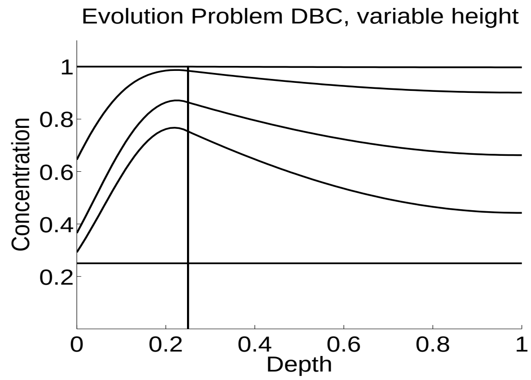

(b) Experiment (2) $u_0 = 0.25$, $m_1 = 20$ and $r = 0.5$.

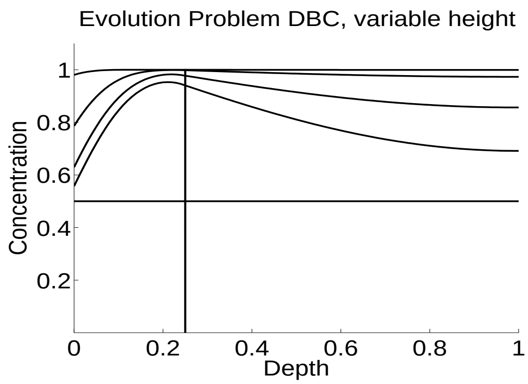

(c) Experiment (3) $u_0 = 0.5$, $m_1 = 20$ and $r = 1$.

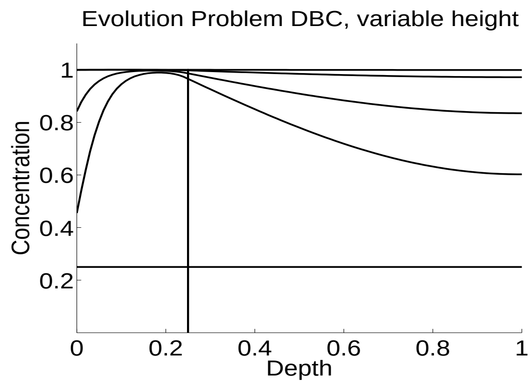

(d) Experiment (4) $u_0 = 0.25$, $m_1 = 200$ and $r = 1$.

Figure 11. Evolution of salt concentration corresponding to Experiments 1-4, for the variable reservoir height problem. Curves correspond to increasingly ordered salt concentration at times, $t \approx 0,\ 5,\ 10,\ 20,\ 40$ years. Vertical line is the roots depth.

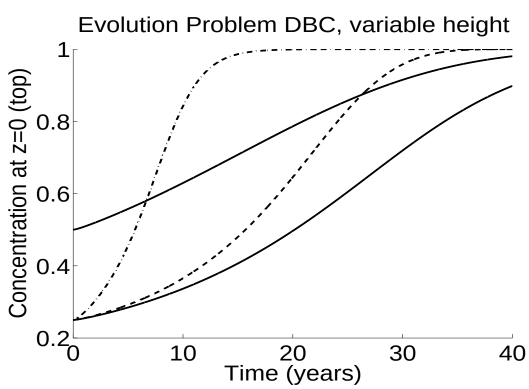

(a) Variable reservoir height problem.

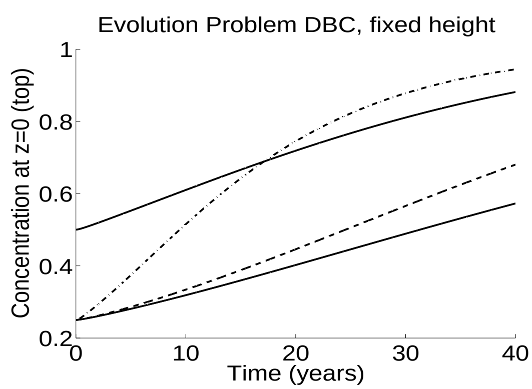

(b) Fixed reservoir height problem.

Figure 12. Evolution of salt concentration on the top boundary corresponding to Experiments 1-4. Continuous line: Experiments 1 and 3. Dotted line: Experiment 2. Point-Dotted line: Experiment 4.

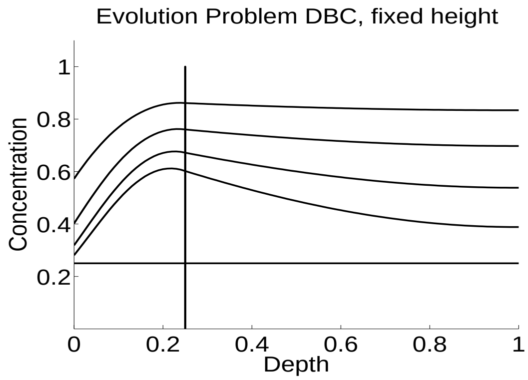

(a) Experiment (1) $u_0 = 0.25$, $m_1 = 20$ and $r = 1$.

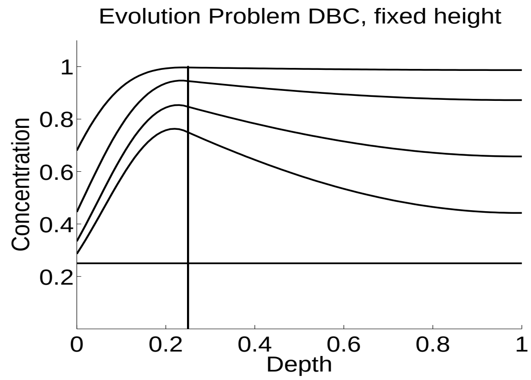

(b) Experiment (2) $u_0 = 0.25$, $m_1 = 20$ and $r = 0.5$.

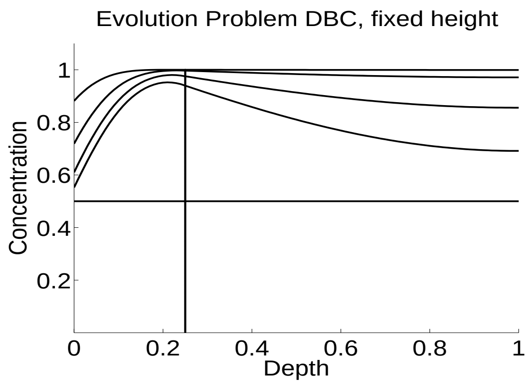

(c) Experiment (3) $u_0 = 0.5$, $m_1 = 20$ and $r = 1$.

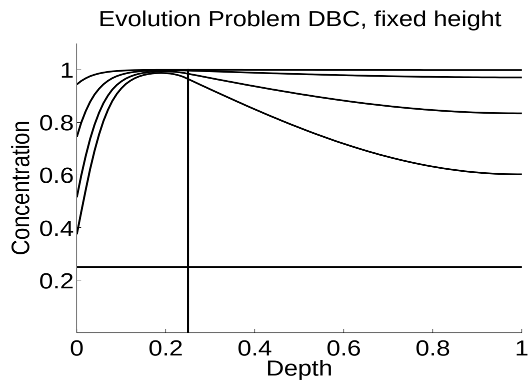

(d) Experiment (4) $u_0 = 0.25$, $m_1 = 200$ and $r = 1$.

Figure 13. Evolution of salt concentration corresponding to Experiments 1-4, for the fixed reservoir height problem. Curves correspond to increasingly ordered salt concentration at times, $t \approx 0,\ 5,\ 10,\ 20,\ 40$ years. Vertical line is the roots depth.

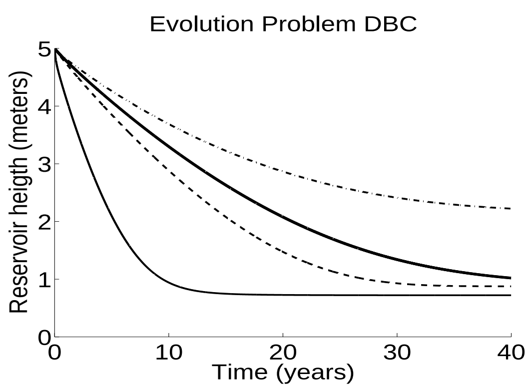

(a) Evolution of the reservoir height.

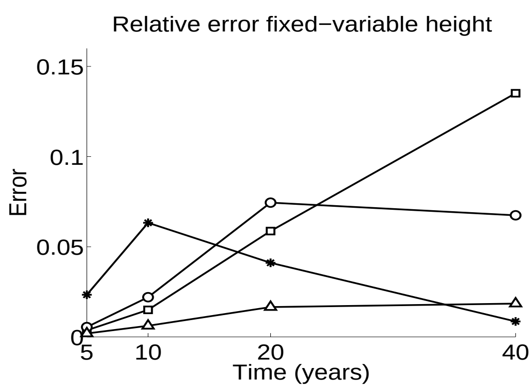

(b) Relative error (203).

Figure 14. (a) Evolution of the reservoir height, w, corresponding to Experiments 1-4. Continuous thick line: Experiment 1. Dotted line: Experiment 2. Point-Dotted line: Experiment 3. Continuous thin line: Experiment 4. (b) Relative error given by (203). Squares, circles, triangles and asterisks correspond to Experiments 1-4, respectively.

5 Full salinization of the root zone

In this section we present a result concerning to the formation of dead cores, i.e., regions in which the threshold level of salt concentration $u = 1$ is attained in finite time, for the solutions of the evolution problems we treated in Sections 2-4. The simplest tool for deducing this type of properties is the comparison principle, which allows to compare solutions of the original problem with solutions of related but simpler problems for which the result is known. We already used this technique for the one-dimensional steady state problem, see Theorem 2

However, since in general the comparison principle is not true for systems of equations, we use an alternative method based on local energy estimates, see the monograph of Antontsev, Díaz and Shmarev [5] on local energy methods for free boundary problems. The method roughly works as follows: first, an energy functional given in terms of norms of the natural energy spaces associated with the problem and which are evaluated in a variable space-time region is introduced. Then, using the partial differential equation satisfied by the solution, a differential inequality for the local energy functional is obtained. Finally, the formation of a dead core is deduced from the properties of solutions to this inequality.

The energy method that we use has two principal features. First, it is a local method, i.e. it operates in subsets of the corresponding domain without need of global informations like boundary conditions or boundedness of the domain. Secondly, it has a very general setting, allowing to consider, for instance, problems in any space dimension or with coefficients depending on the space or time variable. The energy method that we use does not need any monotonicity assumption on the nonlinear functions and it requires no comparison principle.

The method was introduced by Antontsev [2] and developed by J. I. Díaz and Véron in [21] and by Antontsev, J. I. Díaz and Shmarev in [3,4] for parabolic equations of degenerate type. The energy methods have been extended to equations of arbitrary order [11] and have been applied to systems of equations [12, 19, 20, 29, 38]. We refer to [5] for an overview of the existing literature.

Although the method may be applied to systems of equations formulated in a very general form, we shall present it in the simpler one-dimensional formulation for clarity. We first introduce some notation. Performing the change of unknown $w = 1 - u$ in Equations (96) and (97) to remove the singularity from $u = 1$ to $w = 0$, we get

$$w_t + (wv)_z - w_{zz} + m_1 f(z, 1 - w) = 0, \tag{204}$$

$$v_z + m_1 f(z, 1 - w) = 0, \tag{205}$$

in Q_T. For any $t \in (0, T)$ we consider the set

$$\mathcal{P}(t) := \{(z, \tau) : |z - z_0| < R(\tau; t), \quad \tau \in (t, T)\},$$

with $R(\tau; t) := (\tau - t)^\nu$, $0 < \nu < 1$ to be fixed and $z_0 \in (0, 1)$ such that

$$R(T; 0) < z_0 < 1 - R(T; 0),$$

implying $\mathcal{P}(t) \subset Q_T$ for all $t \in (0, T)$, see Figure 15. For brevity, we shall write $\mathcal{P}$ instead of $\mathcal{P}(t)$. We decompose the boundary of $\mathcal{P}$ into final and lateral parts:

$$\partial\mathcal{P}(t) := \partial_f \mathcal{P}(t) \cup \partial_l \mathcal{P}(t),$$

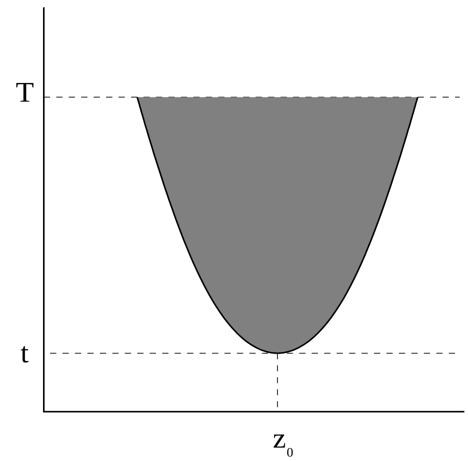

Figure 15. The set $\mathcal{P}(t)$

with $\partial_f \mathcal{P}(t) := \{(z,T) \in \partial\mathcal{P}\}$ and $\partial_l \mathcal{P}(t) := \{(z,\tau) \in \partial\mathcal{P} : t < \tau < T\}$. Finally, we define the *local energy functions*

$$E(t) := \int_{\mathcal{P}(t)} |w_z|^2 \, dz d\tau \quad \text{and} \quad C(t) := \int_{\mathcal{P}(t)} w^{r+1} \, dz d\tau. \tag{206}$$

Concerning function f we assume, in addition to Hypothesis H_2 in page 14, the existence of constants k_0 and k_1 such that

$$0 < k_0 s^{r+1} \leq m_1 s f(\cdot, 1-s) \leq k_1 s^{r+1} \quad \text{for } s \in [0,1] \tag{207}$$

in $\mathcal{P}(t)$ for a.e. $t \in (0,T)$, with $r \in (0,1)$ and $k_0 > k_1/2$.

Theorem 7 *Assume* (207). *Then there exists a positive constant M such that if $E(0) + C(0) \leq M$ then $w \equiv 0$ in $\mathcal{P}(t^*)$, for some $t^* \in (0,T)$.*

Remark 5 (i) *If $f(z,u) = k(z)(1-u)^r$, with k given by (23) then (207) is trivially satisfied in the region where $k \neq 0$.*

(ii) Dirichlet data problem. *Testing equation (204) with w and using (205) and the auxiliary conditions of problem (96)-(99) we obtain the following estimate*

$$E(0) + C(0) \leq \int_\Omega (1 - u_0(z))^2 dz - \int_0^T (1 - u_{top}(t)) u_z(0,t) dt.$$

In some situations, for instance when $u_{top}(t) \leq u_0(z)$ for $t \in (0,T)$ and $z \in (0,1)$, we have $u_z(0,t) \geq 0$ for $t \in (0,T)$, allowing us to obtain an estimate of $E(0) + C(0)$ only in terms of the initial datum. Notice that a typical data is $u_{top} = u_0 =$ constant, for which the above condition is satisfied.

(iii) Dynamic boundary condition problem. *Proceeding as in (ii) but using the boundary conditions of problem (169)-(174) we obtain the estimate*

$$2E(0) + C(0) \leq \int_\Omega (1-u_0)^2 + (1-u_0(0))^2 \big(1 + m_1 \int_{Q_T} f(\cdot,u)\big). \tag{208}$$

Therefore, if the initial datum is close enough to one then the initial energy bound is satisfied. Combining Theorems 6 and 7 we deduce the following corollary.

Corollary 1 *Let (u,v) be a strong solution of problem (169)-(174) in Q_T, for T large enough. Under the conditions of Theorems 6 and 7 there exist $T_0, t^* > 0$ such that $u \equiv 1$ in $\mathcal{P}(t^*)$, for some $t^* \in (T_0, T)$.*

Or, in other words, the threshold value of salt concentration is attained in any compact set contained in the root zone in finite time, independently of the initial condition.

Proof of Theorem 7. The proof consists of three steps.
Step **1.** Multiplying equation (204) by w and integrating in $\mathcal{P}$ gives

$$\int_{\mathcal{P}} \left\{ \tfrac{1}{2}(w^2)_t + \tfrac{1}{2}\left(\left(w^2 v\right)_z + w^2 v_z \right) + \left(|w_z|^2 - (w w_z)_z \right) + m_1 w f(z, 1-w) \right\} dz d\tau = 0.$$

Using the divergence theorem, equation (205) and assumption (207) we find

$$\begin{aligned} \int_{\mathcal{P}} |w_z|^2\, dz d\tau \quad &+ k_0 \int_{\mathcal{P}} w^{r+1}\, dz d\tau \le \int_{\partial_l \mathcal{P}} w w_z n_z\, dz d\tau - \\ &- \tfrac{1}{2} \int_{\partial_l \mathcal{P}} w^2 \left(n_\tau + v n_z\right) dz d\tau + \frac{k_1}{2} \int_{\mathcal{P}} w^{r+2}, \end{aligned}$$

with (n_z, n_τ) the unitary outward normal vector to $\mathcal{P}$, given by

$$(n_z, n_\tau) := \begin{cases} (0,1) & \text{in } \partial_f \mathcal{P}, \\ \frac{\left((\tau - t)^{1-\nu}, -\nu\right)}{\left(\nu^2 + (\tau - t)^{2(1-\nu)}\right)^{1/2}} & \text{in } \partial_l \mathcal{P}. \end{cases}$$

Using $w \le 1$, $v \le k_1$ in Q_T and (n_z, n_τ) unitary we obtain

$$E(t) + (k_0 - \frac{k_1}{2}) C(t) \le \tfrac{1+k_1}{2} I_2(t) + \int_{\partial_l \mathcal{P}} |w|\, |w_z|\, dz d\tau, \tag{209}$$

where we introduced the notation $[w] := |w(z_0 + R(\tau;t), \tau)| + |w(z_0 - R(\tau;t), \tau)|$ and

$$I_2(t) := \int_t^T \left[w^2\right] d\tau.$$

Step **2.** Our aim is to estimate the right hand side of (209) by means of the functions at the left hand side and their derivatives. First notice that

$$\frac{dE}{dt}(t) = \int_t^T \left[|w_z|^2\right] \frac{\partial R}{\partial t}(\tau;t) d\tau,$$

and therefore we can use Hölder's inequality to get

$$\begin{aligned} \int_{\partial \mathcal{P}} |w|\, |w_z|\, dz d\tau \quad &\le \quad \left(\int_t^T -\frac{\partial R}{\partial t} \left[|w_z|^2\right] d\tau \right)^{1/2} \left(\int_t^T \left(-\frac{\partial R}{\partial t} \right)^{-1} \left[w^2\right] d\tau \right)^{1/2} = \\ &= \quad I_1(t) \left(-\frac{dE}{dt}(t) \right)^{1/2} \le I_1(t) \left(-\frac{d\,(E + C)}{dt}(t) \right)^{1/2}, \end{aligned} \tag{210}$$

with

$$I_1(t) := \left(\int_t^T \left(-\frac{\partial R}{\partial t} \right)^{-1} \left[w^2 \right] d\tau \right)^{1/2}.$$

To handle $I_1(t)$ and $I_2(t)$ of (209) we shall apply a simple version of an interpolation-trace inequality. A proof of this particular result may be found in [22]. See [5] for a more general version.

Lemma 6 *Let* $\varphi \in H^1(z_0-\rho, z_0+\rho)$, *for* $z_0 \in \mathbb{R}$ *and a positive constant* ρ. *Then*

$$|\varphi(z_0-\rho)| + |\varphi(z_0+\rho)| \le L_0 \left(\|\varphi_z\|_2 + \rho^{-\delta} \|\varphi\|_{r+1} \right)^{\gamma} \|\varphi\|_r^{1-\gamma}, \tag{211}$$

with $L_0 \le 16$, $\beta \in [1,2]$, $r \ge 0$,

$$\gamma = \frac{2}{2+\beta} \quad \textit{and} \quad \delta = \frac{r+3}{2(r+1)}. \tag{212}$$

Here we used the notation $\|\cdot\|_s := \|\cdot\|_{L^s(z_0-\rho, z_0+\rho)}$. We take $\beta < 2$ and find, by applying Hölder's inequality with exponent $\theta := \frac{1-r}{2-\beta}$

$$\|\varphi\|_\beta \le \|\varphi\|_2^{\frac{2}{\beta\theta'}} \|\varphi\|_{r+1}^{\frac{r+1}{\beta\theta}}, \tag{213}$$

where we have used the notation $\theta' = \theta/(\theta-1)$. Combining (211) and (213) with $\varphi(z) := w(z,\tau)$ and using $w \le 1$ we get

$$\left[w^2 \right] \le [w]^2 \le L_0^2 m(R) \left(\|w_z\|_2^2 + \|w\|_{r+1}^{r+1} \right)^{\gamma} |Q_T|^{\frac{2(1-\gamma)}{r\theta'}} \|w\|_{r+1}^{\frac{2(1-\gamma)(r+1)}{\beta\theta}} \tag{214}$$

with $m(R) := \max\left\{1, R^{-2\delta\gamma}\right\}$. We then deduce from (214)

$$I_1(t) \le L_0 |Q_T|^{\frac{1-\gamma}{\beta\theta'}} \left(\int_t^T m(R) \left(-\frac{\partial R}{\partial t} \right)^{-1} \left(\|w_z\|_2^2 + \|w\|_{r+1}^{r+1} \right)^{\gamma + \frac{2(1-\gamma)}{\beta\theta}} d\tau \right)^{1/2}. \tag{215}$$

Due to the crucial assumption $r < 1$, it is compatible to choose $\beta < 2$ and $\beta \ge \frac{4}{3-r}$. Then we obtain that μ given by

$$\mu^{-1} := \gamma + \frac{2(1-\gamma)}{\beta\theta} \tag{216}$$

satisfies $\mu \ge 1$. Using Hölder's inequality with exponent μ and substituting the explicit expression of R we obtain from (215)

$$I_1(t) \le \Lambda(t) \left(E(t) + C(t) \right)^{\frac{\gamma}{2} + \frac{1-\gamma}{\beta\theta}}, \tag{217}$$

with

$$\Lambda(t) := L_0 |Q_T|^{\frac{1-\gamma}{\beta\theta'}} \nu^{-1/2} \left(\int_t^T (\tau - t)^{\mu'(1-\nu-2\delta\nu\gamma)} d\tau \right)^{1/2\mu'}. \tag{218}$$

Function Λ is finite whenever we choose $\nu < \frac{\mu+1}{\mu(1+2\delta)}$ which is always possible since the only restriction assumed on ν is $0 < \nu < 1$. Gathering (210) and (217) we get

$$\int_{\partial\mathcal{P}} |w|\,|w_z|\,dz d\tau \leq \Lambda(t)\left(-\frac{d\,(E+C)}{dt}(t)\right)^{1/2}(E(t)+C(t))^{\frac{\gamma}{2}+\frac{1-\gamma}{\beta}}. \tag{219}$$

In a similar way, but choosing $\beta = 2$ in (211), we get the following estimate

$$I_2(t) \leq L_0\Gamma(t)\,(E(t)+C(t)), \tag{220}$$

with $\Gamma^2(t) := \int_t^T (\tau - t)^{-\delta\nu} d\tau < \infty$ if $\nu < 1/\delta$.
Step **3.** From (209), (215) and (220) we deduce

$$c_0(E(t)+C(t)) \leq \Lambda(t)\left(-\frac{d\,(E+C)}{dt}(t)\right)^{1/2}(E(t)+C(t))^{\frac{\gamma}{2}+\frac{1-\gamma}{\beta}},$$

with $c_0 \leq k_0 - \frac{k_1}{2} - \frac{1+k_1}{2}L_0\Gamma(t)$. Notice that making $T-t$ small enough, say $T-t \leq \varepsilon$, we can ensure $c_0 > 0$. Making the assumption, to force a contradiction, that $E(t)+C(t) > 0$ for all $t \in [0,T]$, we arrive at the inequality

$$c_0^2\,(E(t)+C(t))^{2\left(1-\frac{\gamma}{2}-\frac{1-\gamma}{\beta}\right)} \leq -\Lambda(t)^2\frac{d\,(E+C)}{dt}(t). \tag{221}$$

Due again to $r < 1$ we find $\sigma := 2\left(1-\frac{\gamma}{2}-\frac{1-\gamma}{\beta}\right) < 1$. We assume $T > \varepsilon$ and restrict t to take values on $(T-\varepsilon, T)$ (so $T-t \leq \varepsilon$ is fulfilled). Integrating (221) in $t \in (T-\varepsilon, t^*)$ with $t^* \in (T-\varepsilon, T)$ we obtain

$$(E+C)^{1-\sigma}(t^*) \leq (E+C)^{1-\sigma}(T-\varepsilon) - (1-\sigma)c_0^2\int_{T-\varepsilon}^{t^*}\Lambda(t)^{-2}dt.$$

Therefore, since $E+C$ is non-increasing we have that if the initial energy satisfies

$$(E+C)^{1-\sigma}(0) \leq (1-\sigma)c_0^2\int_{T-\varepsilon}^{t^*}\Lambda(t)^{-2}dt =: M^{1-\sigma}$$

then $E(t^*)+C(t^*) = 0$, which is the announced contradiction. Therefore, there exists some $t^* \in (0,T)$ such that $E(t)+C(t) > 0$ for all $t > t^*$, implying $w = 0$ in $\mathcal{P}(t^*)$. □

6 Conclusion

In this chapter we have introduced and analyzed a model for the description of the salt concentration evolution and water motion induced by the salt exclusion mechanisms of mangrove roots. This description was formulated in terms of a system of partial differential equations inspired on that introduced by Passioura et al. [47]. However, we incorporated major generalizations in several directions. First, we considered the global scenario of a water-soil domain, in which a layer of saline water, such as in backwaters or marshes, lies over a saturated porous medium where the mangroves grow. The appropriate mathematical model for this physical situation is the so called Stokes-Darcy model together with an evolution convection-diffusion partial differential equation for the salt concentration.

We deduced a dimensionless formulation in which there appeared three dimensionless numbers capturing the relevant physical aspects of the problem: a Rayleigh number, measuring the ratio hydraulic conductivity-molecular diffusion, a extraction number, measuring the ratio mangroves transpiration rate-hydraulic conductivity, and a “viscosity” number, proportional to permeability. We checked that, under usual conditions, the latter is very small compared to the formers and may be neglected in a first approximation. The implication is that the water-soil model may be simplified in this usual situations, where only the soil domain may be considered. Naturally, this soil model is also the adequate for other typical situations in which mangroves grow on terrains which are only periodically inundated. However, in unusual situations such as that discussed in Section 4, where the natural water circulation in a marsh was impeded, the whole system should be taken into account. Consequently, we started our discussion proving the well posedness of the mathematical problem in the more general water-soil domain situation. As a matter of fact, this proof is also valid for the soil model under minor modifications.

We dedicated Section 3 to the study of the soil model. Starting with the simplest situation in which only the vertical coordinate, the depth, is considered, we were able to prove several quantitative and qualitative properties of the mathematical model such as the uniqueness and comparison of solutions, which allowed us to establish the connection between the solutions of the time-dependent problem and the steady state problem, as well as the property of formation of a dead core, or fully salinized region, and the stability of the one-dimensional time-dependent solution. We also introduced numerical schemes to approximate the solutions and tested them with typical values of the physical parameters. In our numerical experiments we checked the importance of the functional form of the extraction function for the formation of dead cores. However, although mathematically interesting, we demonstrated that the product of the Rayleigh number times the extraction number, which captures the ratio transpiration rate-molecular diffusion, is the most important and physically understandable parameter of the model. We also checked that the actual value of salt concentration at the surface is not significant for the resulting salt concentration in the subsurface, except for the first few centimeters of the roots.

Our investigation on the stability of the solution of the one-dimensional problem was motivated by the observation of a potential instable situation which arises in the first stages of the evolution profile of the solution. Indeed, the salt exclusion mechanisms of mangroves produce a layer of heavier water around the roots over a layer of lighter water below them. We proved analytically (for a related problem) and demonstrated numerically that this configuration is instable if the permeability of the porous medium and, therefore, its hydraulic conductivity, is high enough. If such is the case, the formation of transient Bénard cells speeds up the mixing of the salt in the porous medium, resulting in a faster convergence to the steady state than that predicted by the one-dimensional model.

In Section 4 we deduced a water-soil model for stagnant water conditions. Although related to the general model, we re-level the mathematical difficulties by allowing a moving boundary (the top of the water domain) but under the assumption of a uniform salt concentration in the water reservoir. After applying the water and salt mass conservation principles we deduced a problem for the soil domain with a new kind of boundary condition: a dynamic boundary condition. We proved the mathematical well-posedness of the problem and stated some of its properties. It is interesting to observe that the salt concentration tends to the threshold level in the whole domain, capturing the situation in which mangroves mechanisms of salt extrusion drive theirselves to death (in few years) when the natural water circulation conditions are impeded.

Finally, in Section 5 we investigated the possibility that the salt exclusion mechanisms may (locally) bring the water uptake to a complete standstill due to the increase of the salt concentration until the threshold mangroves tolerance level is reached. This is a common feature to all the models studied in this chapter and, in mathematical terms, depends on the functional form of the extraction function. Since the mathematical proof is quite involved and technical we presented the smoother version of the one-dimensional problem. The results that we analytically proved in this section were numerically demonstrated along the previous sections of the chapter.

References

[1] Alt, W. & Luckhaus, S. (1983). Quasilinear elliptic-parabolic differential equations, *Math. Z., 183*, 311-341.

[2] Antontsev, S. N. (1981). On the localization of solutions of nonlinear degenerate elliptic and parabolic equations. *Sov. Math. Dokl., 24*, 420-424.

[3] Antontsev, S. N. & Díaz, J. I. (1991). Space and time localization in the flow of two immiscible fluids through a porous medium: energy methods applied to systems. *Nonlin. Anal., 16*, 299-313.

[4] Antontsev, S. N., Díaz, J. I. & Shmarev, S. (1995). The support shrinking in solutions of parabolic equations with nonhomogeneous absorption terms. *Ann. Fac. Sci. Toulouse, VI. Ser., Math. 4*, 5-30.

[5] Antontsev, S. N., Díaz, J. I., & Shmarev, S. (2002). *Energy methods for free boundary problems.* Boston, USA: Birkhäuser.

[6] Arino, O., Gauthier, S. & Penot, J. P. (1987). A fixed point theorem for sequentially continuous mappings with application to ordinary differential equations. *Funkcial Ekvac., 24*, 273–279.

[7] Ball, M. C. (1988). Salinity tolerance in the mangroves *Aegiceras corniculatum* and *Avicennia marina*. I. Water use in relation to growth, carbon partitioning and salt balance, *Aust. J. Plant Physiol, 15*, 447-464.

[8] Bear, J. (1972). *Dynamics of fluids in porous media*. New York, USA: American Elsevier.

[9] Beavers, G. & Joseph, D. (1967). Boundary conditions at a naturally impermeable wall, *J. Fluid. Mech., 30*, 197-207.

[10] Bejenerau, I., Díaz, J. I. & Vrabie, I. I. (2001). An abstract approximate controlability result and applications to elliptic and parabolic systems with dynamic boundary conditions, *Elec. J. Diff. Eq., 50*, 1-19.

[11] Bernis, F. (1984). Compactness of the support for some nonlinear elliptic problems of arbitrary order in dimension n. *Comm. P. D. E., 9*, 271-312.

[12] Bernis, F. (1996) Finite speed of propagation and continuity of the interface of thin viscous films. *Adv. Diff. Eqs., 1*, 337-368.

[13] Botero, L. (1990). Massive mangrove mortality of the Caribbean coast of Colombia, *Vida Silve. Neot., 2*, 77-78.

[14] Brezis, H. (1987). *Analise Fonctionnelle. Theorie et applications*, Paris, France: Masson.

[15] Brezzi, F. & Fortin, M. (1991). *Mixed and hybrid finite element methods*. Springer Series in Computational Mathematics, 15, New York, USA: Springer-Verlag.

[16] Brezzi, F., Hughes, T. J. R., Marini, L. D. & Masud, A. (2005). Mixed discontinuous Galerkin methods for Darcy flow, J. Sci. Comput., 22/23, 119-145.

[17] Courant, R. & Hilbert, D. (1965). *Methoden der Mathesmatischen Physik II*, Berlin, Germany: Springer.

[18] Díaz, J. I. (1985). *Nonlinear partial differential equations and free boundaries. Volume I: Elliptic equations.* Research notes in mathematics. London, UK: Pitman.

[19] Díaz, J. I. & Galiano, G. (1997). On the boussinesq system with non linear thermal diffusion. *Nonlin. Anal., 30(6)*, 3255-3263.

[20] Díaz, J. I., Galiano, G., & Jüngel, A. (1999) On a quasilinear degenerate system arising in semiconductor theory. Part II: Localization of vacuum solutions. *Nonlin. Anal., 36(5)*, 569-594.

[21] Díaz, J. I. & Veron, L. (1985). Local vanishing properties of solutions of elliptic and parabolic quasilinear equations. *Trans. Amer. Math. Soc., 290, 2*, 787-814.

[22] van Duijn, C. J., Galiano, G. & Peletier, M. A. (2001) A diffusion-convection problem with drainage arising in the ecology of mangroves. *Interfaces and free boundaries, 3*, 15-44.

[23] van Duijn, C. J., Galiano, G. & Velasco, J. (2009). Existence of solutions and stability analysis for a Darcy flow with extraction. *Nonlinear Anal. RWA, 10(4)*, 2007-2020.

[24] van Duijn, C. J., Pieters, G. J. M., Wooding, R. A. & van der Ploeg, A. (2002). Stability criteria for the vertical bundary layer formed by throughflow near the surface of a porous medium. In P.A.C. Raats, D. Smiles & A.W. Warrick (Eds.), *Geophys. Monographs, Vol. 129*, American Geophysical Union, pp. 155-169.

[25] Escher, J. (1993) Quasilinear parabolic systems with dynamical boundary conditions. *Commun. in Partial Differential Equations, 18*, 1309-1364.

[26] Feller, W. (1952). The parabolic differential equations and the associated semi-groups of transforms. *Ann. of Math., 55*, 468-519.

[27] Filo, J. & Luckhaus, S. (1999). Modelling surface runoff and infiltration of rain by an elliptic-parabolic equation coupled with a first order equation on the boundary. *Arch. Ration. Mech. Anal., 146*, 157-182.

[28] Friedman, A. & Shinbrot, M. (1968). The initial value problem for the linearized equations of water waves. *J. Math. Mech., 17*, 107-180.

[29] Galiano, G. & Peletier, M. A. (1997). Spatial localization for a general reaction-diffusion system. *Ann. Fac. Sci. Toulouse, 7(3)*, 419-441.

[30] Galiano, G. & Velasco, J. (2006). On a dynamical boundary value problem arising in the ecology of mangroves. *Nonlin. Anal., RWA, 7(5)*, 1129-1144.

[31] Gaganis, P., Skouras, E. D., Theordoropoulou, M. A., Tsakiroglou, C. D. & Burganos, V. N. (2005) On the evaluation of dispersion coefficients from visualization experiments in artificial porous media. *J. Hydrology, 307*, 79-91.

[32] González, E. (1991). El manglar de la Ciénaga Grande de Santa Marta, ecosistema en peligro de extinción. *Colombia, sus gentes y regiones, 21*, 2-21.

[33] Gill, A. M. & Tomlinson, P. B. (1977). Studies on the growth or red manrove (*Rizophora mangle* L.) 4. The adult root system. *Biotropica, 9*. 145-155.

[34] Hollins, S. E., Ridd, P. V. & Read, W. W. (2000). Measurement of the diffusion coefficient for salt in salt flat and mangrove soils. *Wetlands Ecology and Management, 8*, 257-262.

[35] Hutchings, P. & Saenger, P. (1987). *Ecology of mangroves*. Queensland, Australia: University of Queensland Press.

[36] Jäger, W. & Mikelić, A. (2000). On the interface boundary condition of Beavers, Joseph and Saffman, *SIAM J. Appl. Math., 60*, 1111-1127.

[37] Kačur, J. (1980). Nonlinear parabolic equations with the mixed nonlinear and nonstationary boundary conditions. *Math. Slovaca, 30*, 213-237.

[38] Kersner, R. & Shishkov, A. (1996). Instantaneous shrinking of the support of energy solutions. *J. Math. Anal. Appl., 198*, 729–750.

[39] Ladyzenskaya, O. A., Solonnikov, V. A. & Ural'ceva, N. N. (1968). *Quasilinear Equations of Parabolic Type*, Translations of Mathematical Monographs, **23**, Providence, USA: American Mathematical Society.

[40] Layton, W., Schieweck, F. & Yotov, I. (2002). Coupling fluid flow with porous media flow. *SIAM J. Numer. Anal., 40*, 2195-2218.

[41] Langlais, M. & Phillips, D. (1985). Stabilization of solutions of nonlinear and degenerate evolution equations. *Nonlinear Anal., 9(4)*, 321-333.

[42] Lin, G. & Stenberg, L. da S. L. (1994). Utilization of surface water by red mangrove (*Rhizophora Mangle L.*): an isotopic study. *Bull. Mar. Sci., 54*, 94-102.

[43] Lions, J. L. (1969). *Quelques méthodes de résolution des problèmes aux limites non linéaires*. Paris, France: Dunod, Gauthiers-Villars.

[44] Lions, J. L. & Magenes, E. (1972). *Nonhomogeneous boundary value problems and applications, Vol. 1*. New York, USA: Springer.

[45] Masud, A. & Huges, T. (2002) A stabilized mixed finite element method for Darcy flow. *Comput. Methods Appl. Mech. Engrg, 191*, 4341-4370.

[46] Paliyavuth, C., Clough, B. & Patanaponpaiboon, P. (2004). Salt uptake and shoot water relations in mangroves. *Aquatic Botany, 78*, 349-360.

[47] Passioura, J. B., Ball, M. C. & Knight, J. H. (1992). Mangroves may salinize the soil and in so doing limit their transpiration rate. *Funct. Ecol., 6*, 476-481.

[48] Payne, L. E. & Straughan, B. (1998). Analysis of the boundary condition at the interface between a viscous fluid and a porous medium and related modelling questions. *J. Math. Pures Appl., 77(9)*, 317-354.

[49] Peddie, W. (1901). Note on the cooling of a sphere in a mass of well stirred liquid. *Proc. Edimburgh Math. Soc., 19*, 34-35.

[50] Perdomo, L., Ensminger, I., Espinosa, L. F., Elster, C., Wallner-Kersanach, M. & Schnetter, M. L. (1998). The mangrove ecosystem of the Ciénaga Grande de Santa Marta (Colombia): Observations on regeneration and trace metals in sediment. *Marine Pollution Bull., 37*, 393-403.

[51] Primicerio, M. & Rodrigues, J. F. (1993). The Hele-Shaw problem with nonlocal injection condition, in *Nonlinear Mathematical Problems in Industry*, Gatuko, Tokyo, 1993.

[52] Saffman, P. (1971). On the boundary condition at the surface of a porous media, *Stud. Appl. Math., L*, 93-101.

[53] Selberher, S. (1984). *Analysis and simulation of semiconductor devices*. Wien, Austria: Springer.

[54] Simon, J. (1987). Compact sets in the space $L^p(0,T;B)$. *Ann. Math. Pures et Appl., 146*, 65-96.

[55] Solonnikov, V. A. & Frolova, E. V. (2000). L^p-theory for the Stefan problem. *J. Math. Sci.*, 989-1006.

[56] Straughan, B. (2004). *The energy method, stability and nonlinear convection*, Applied Mathematical Sciences, 91. New York, USA: Springer-Verlag.

[57] Straughan, B. (2008). *Stability and wave motion in porous media*, Applied Mathematical Sciences, 165. New York, USA: Springer-Verlag.

[58] Thomas. J. M. (1977). *Sur l'analyse numérique des méthodes d'éléments finis hybrides et mixtes*, Thèse de Doctorat d'etat, Université Pierre et Marie Curie (Paris 6), Paris, France.

[59] Tomlinson, P. B.(1986). *The Botany of Mangroves.* Cambridge, U.K.: Cambridge University Press.

[60] Rappoldt, C., Pieters, G. J. M., Adema, E., Baaijens, G. J. & van Duijn, C. J. (2003). Buoyancy-driven flow in a peat moss layer as a mechanism for solute transport. *Proc. Natl. Acad. Sci. USA, 100*, 14937-14942.

[61] Wolfram Research Inc., Mathematica® .